On the Macroscopic Modeling of Dilute Emulsions Under Flow in the Presence of Particle Inertia

P. Masafu Mwasame, Norman J. Wagner, Antony N. Beris[a)]

Center for Molecular and Engineering Thermodynamics, Department of Chemical and Biomolecular Engineering, University of Delaware,

Newark, DE 19716, USA

[a)]Corresponding Author. Tel. 1- 302- 831-8018, E-mail address: beris@udel.edu

Proposed Journal: Physics of Fluids

Recently, Mwasame *et al.* (J. Fluid Mech., vol. 831, 2017, p. 433) developed a macroscopic model for the dynamics and rheology of a dilute emulsion with droplet morphology in the limit of negligible particle inertia using the bracket formulation of non-equilibrium thermodynamics of Beris and Edwards (Oxford U. Press, 1994). Here, we improve upon that work to also account for particle inertia effects. This advance is facilitated by using the bracket formalism in its inertial form that allows for the natural incorporation of particle inertia effects into macroscopic level constitutive equations while preserving consistency to the previous inertialess approximation in the limit of zero inertia. The parameters in the resultant Particle Inertia Thermodynamically Consistent Ellipsoidal Emulsion (PITCEE) model are selected by utilizing literature-available mesoscopic theory for the rheology at small Capillary and particle Reynolds numbers. At steady-state, the lowest level particle inertia effects can be described by including an additional non-affine inertial term into the evolution equation for the conformation tensor, thereby generalizing the Gordon-Schowalter time derivative. This additional term couples the conformation and vorticity tensors and is a function of the Ohnesorge number. The rheological and microstructural predictions arising from the PITCEE model are compared against steady-shear simulation results from literature. They show a change in the signs of the normal stress differences that is accompanied by a change in the orientation of the major axis of the emulsion droplet towards the velocity gradient direction with increasing Reynolds number, capturing the two main signatures of particle inertia reported in simulations.

I. INTRODUCTION

An important and common assumption in continuum macroscopic models of complex fluids and soft material flow and dynamics is that microscopic particle inertia effects are negligible. Physically, this means that the divergence of the extra stress tensor is independent of the acceleration of the system and thus, of any solid body rotation. Mathematically, this requires the extra stress expression, if it is explicitly obtained in terms of the local kinematics, to only involve the symmetric rate of strain component of the velocity gradient tensor. Such is the case for generalized Newtonian fluid flow models. For many complex fluids, the stress tensor is obtained implicitly in terms of a contravariant or covariant second order tensor, depending on the choice of the microstructural descriptor. In such models, material objectivity and Galilean invariance require only the involvement of very specific contributions of symmetric (rate-of-strain) and anti-symmetric (vorticity) components of the velocity gradient in defining the upper or lower convected time derivatives respectively[1]. Requiring the extra stress tensor to be invariant to solid body rotation also explains why the only allowed, non-affine corrections to the upper convected time derivative involve the rate-of-strain tensor. This explains the absence of the vorticity tensor from the non-affine correction to the upper convected derivative that gives rise to the Gordon-Schowalter derivative[2, 3]. However, although microstructural inertia is typically negligible under most typical circumstances, this is not always the case. Of particular interest to this work is when the particle Reynolds number, selected based on a characteristic microscopic particle length scale, becomes of the order of one-tenth or higher, in which case particle inertia effects become important[4-6].

Considerable progress has already been made towards developing rheological models for emulsions in the absence of particle scale inertia. These developments have been made through either phenomenological approaches[7-10] or more formally by applying the framework of Non-Equilibrium Thermodynamics[11-16]. Regardless of the approach, the key modeling consideration is that the microstructure of an emulsion droplet can be represented using a second order tensor. However, of the two approaches, the NET framework is preferred because the corresponding constitutive relationship for the stress tensor emerges self-consistently. A more thorough literature survey of current progress in emulsion flow modeling can found in Minale[17] and Mwasame *et al*.[18]. Recently, there has been a renewed interest in understanding the effects of particle-scale inertia in suspensions[19-21] and emulsions with droplet morphology[22-25]. An important observation in simulation studies involving particle-scale inertia in emulsions[22] is the emergence of a negative first normal stress difference (N_1) and a positive second

normal stress difference (N_2). This is in contrast with inertialess emulsion flow theory[26, 27] that predicts a positive N_1 and negative N_2. Furthermore, in the same simulation studies[22] at non-zero particle Reynolds number, the deformed droplets are observed to increasingly orient in the direction of the velocity gradient in shear flows. This orientation is in direct contrast to experimental studies in the absence of inertia where droplets orient increasingly in the flow/velocity direction[28]. Such complex and non-intuitive phenomena are the motivation for developing new macroscopic flow models that take particle inertia effects into account.

The ubiquity of complex fluids in a wide variety of process flow conditions justifies the need to develop new capabilities within macroscopic models to account for the rheological phenomena associated with particle inertia. Unlike secondary flow effects, for example, turbulence arising due to the choice of the external flow conditions and geometry[29], particle-scale effects leading to micro-inertia may be considered an intrinsic property of a complex fluid as they do not depend on a macroscopic length scale. The scaling of particle inertia effects involves a microscopic length ℓ that enters the definition of the particle Reynolds number, Re_p. Micro-inertia effects can be neglected if the particle Reynolds number is small, as for example in the bulk, laminar flow of molecular fluids and nanoparticle dispersions. On the other hand, for complex fluids with supermolecular structures, such as suspensions of micron-scale or larger rigid spheres, aggregates or emulsions, a particle Reynolds number of order one tenth or larger may be realized indicating micro-inertia effects are important[4-6]. Under these conditions, the distorted microscale flow around the supermolecular structure may be highly non-linear and characterized by boundary layer separation, as shown in the highly idealized depiction of an emulsion droplet in Fig. 1. This distinguishes particle scale inertia from inertial effects traditionally associated with macroscopic turbulence and opens a promising new application area for conformation tensor-based macroscopic continuum models.

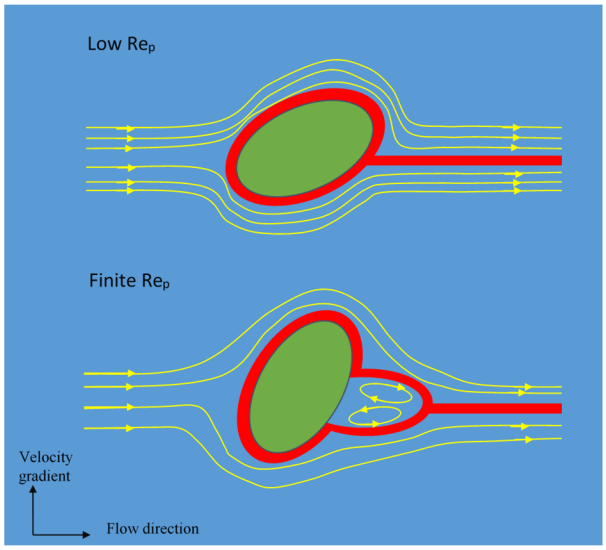

Figure 1: An idealized schematic depiction of micro-inertia effects on a single emulsion droplet in material flow. In the presence of micro-inertia, the droplet increasingly orients in the direction of the velocity gradient in a shear flow. Bold (red) lines are a depiction of the boundary layer surrounding the deformed droplet/ellipsoid.

Emulsions with droplet morphology are a particularly useful case study to understand the effects of micro-inertia since they are easily amenable to continuum level modeling through conformation tensor-based models[7, 9, 18]. Mwasame *et al.*[18] have outlined a particularly useful Thermodynamically Consistent Emulsion Ellipsoidal (TCEE) model that distinguishes itself by being consistent with known asymptotic theories for small Capillary numbers, but at zero particle Reynolds for dilute emulsions with droplet morphology[26, 27, 30-32]. Despite this latest advance, developing macroscopic models for emulsion rheology for non-zero, even small, particle Reynolds numbers remains an open question. Recent studies using both simulation[22] and theoretical[23] investigations to understanding the rheology of dilute emulsions at finite particle Reynolds numbers provide an ideal setting to understand and advance new macroscopic models for emulsion rheology when micro-inertia is present.

So far, the only other macroscopic flow models in which microscopic inertial effects have been taken into account are those for liquid crystalline systems, which were actually first developed in an inertial form[33, 34]. Subsequently, the non-inertial forms were developed as approximations in the limit of zero inertia and both forms have been consistently expressed within the bracket formulation of Non-Equilibrium Thermodynamics[35]. Although Dressler[36] attempted to adapt the same framework applied towards tensor-based constitutive models for liquid crystalline systems to emulsions in inertial flows, his efforts remain incomplete as he failed in his equations to account for the more complex, anisotropic, dissipation relaxation behavior encountered in the latter. The general lack of conformation tensor models

in which inertial effects are taken into account may stem from the current applications of such models to systems and for process conditions under which particle inertia effects are negligible. However, as new applications emerge, for example involving microfluidic devices under high Reynolds number conditions and/or particle-based systems with large enough particle sizes (developed for example through aggregation), micro-inertial effects may become significant.

Recent theoretical and simulation work[22, 23] on emulsion rheology suggests that inertial effects, though subtle, may be more prevalent than previously thought, such that effects appear at a particle Reynolds number as low as 0.1. The main goal of this work to capitalize on the capability of the bracket approach to naturally describe particle inertia effects directly into material flow models. This allows for the derivation of inertial macroscopic models fully capable of predicting the key micro-inertia effects in dilute emulsions as revealed by the recent numerical and simulation studies previously mentioned. Furthermore, the recently developed inertialess macroscopic model for dilute emulsion through the bracket formulation (TCEE model) is utilized to provide an important limiting case to fix model parameters and ensure the consistency of the micro-inertial emulsion model against its micro-inertialess limit. This is developed here within the same rigorous thermodynamically-consistent bracket NET framework, giving rise to the so-called Particle Inertia Thermodynamically Consistent Ellipsoidal Emulsion (PITCEE) model.

In the next section, we outline the latest literature-available microscopic theory results for the shear stress of a dilute emulsion at small non-zero particle Reynolds numbers. In section III, we present the general development, through the single generator bracket approach of Non-Equilibrium Thermodynamics[35], of the micro-inertial emulsion flow (PITCEE) model. In section IV, we explain how the literature-available microscopic theories in the limit of small Reynolds and Capillary numbers, are used both to provide independent validation of the final macroscopic equations and to determine the PITCEE model parameters. In section V, we compare the PITCEE model predictions against existing simulation results for the rheology and droplet morphology of single emulsion droplets in the presence of inertia. Finally, in section VI we present our conclusions.

II. PREVIOUS MICROSCOPIC THEORY AND SIMULATIONS AT FINITE PARTICLE INERTIA IN THE LITERATURE

Microscopic theory and simulations provide important independent results to rigorously examine the consistency of macroscopic models. This has been successfully demonstrated in the recent work of Mwasame *et al.*[18] in relation to the development of the TCEE model in the limit of zero particle Reynolds

number flows when asymptotic results available for small Capillary numbers but zero particle inertia were used. The recent asymptotic theory by Raja *et al.*[23] on the rheology of dilute emulsions in the presence of micro-inertia provides important results that are useful for parameterizing and validating corresponding macroscopic micro-inertial emulsion flow models. More specifically, the expression for the extra stress for a general linear flow field in the limit of small Capillary and Reynolds numbers is given by[23]

$$\underline{\underline{\sigma}} = 2\mu\left(1+\phi\left(\frac{5\lambda+2}{\lambda+1}\right)\right)\underline{\underline{D}} - \phi Ca^{*}\mu\left\{\begin{array}{l}\frac{1}{40}\left(\frac{19\lambda+16}{\lambda+1}\right)^{2}\left(\frac{D}{Dt}\underline{\underline{D}}-\left(\underline{\underline{\Omega}}\cdot\underline{\underline{D}}-\underline{\underline{D}}\cdot\underline{\underline{\Omega}}\right)\right)+ \\ \frac{3(19\lambda+16)\left(25\lambda^{2}+41\lambda+4\right)}{140(\lambda+1)^{3}}\left(\underline{\underline{D}}\cdot\underline{\underline{D}}-\frac{1}{3}\mathrm{tr}\left(\underline{\underline{D}}\cdot\underline{\underline{D}}\right)\underline{\underline{I}}\right)\end{array}\right\}. \quad (1)$$

$$+\phi Re_{p}^{*}\mu\left\{\frac{\left(27\lambda^{2}+30\lambda+10\right)}{(\lambda+1)^{2}}\frac{D}{Dt}\underline{\underline{D}}-\frac{4\left(3\lambda^{2}+3\lambda+1\right)}{9(\lambda+1)^{2}}\left(\underline{\underline{\Omega}}\cdot\underline{\underline{D}}-\underline{\underline{D}}\cdot\underline{\underline{\Omega}}\right)\right\}+\ldots$$

where $\lambda \equiv \mu_d / \mu$ is the viscosity ratio (with μ_d the droplet viscosity and μ is the matrix viscosity), $Ca^{*} \equiv \mu a / \gamma$ (with a the droplet radius, . γ . the surface tension and μ is the medium viscosity) and $Re_p^{*} \equiv a^2 \rho / \mu$ (with ρ is the density) are characteristic time scales that, when scaled by the flow time scale taken as the inverse of the shear rate $\dot{\gamma}$, lead to the Capillary and particle Reynolds numbers, $Ca \equiv \mu a \dot{\gamma} / \gamma$ and $Re_p \equiv a^2 \rho \dot{\gamma} / \mu$, respectively. In the same expression, the rate of strain tensor, $\underline{\underline{D}}$, is defined as

$$\underline{\underline{D}} \equiv \frac{1}{2}\left(\left(\underline{\nabla V}\right)^{T}+\left(\underline{\nabla V}\right)\right), \quad (2)$$

while the vorticity tensor, $\underline{\underline{\Omega}}$, is defined as

$$\underline{\underline{\Omega}} \equiv \frac{1}{2}\left(\left(\underline{\nabla V}\right)^{T}-\left(\underline{\nabla V}\right)\right), \quad (3)$$

respectively. For shear flows, with the flow, shear and vorticity directions being identified as directions 1, 2 and 3, respective these two tensors reduce to

$$\underline{\underline{D}} = \frac{1}{2}\begin{bmatrix} 0 & \dot{\gamma} & 0 \\ \dot{\gamma} & 0 & 0 \\ 0 & 0 & 0 \end{bmatrix}, \quad (4)$$

and

$$\underline{\underline{\Omega}} = \frac{1}{2}\begin{bmatrix} 0 & \dot{\gamma} & 0 \\ -\dot{\gamma} & 0 & 0 \\ 0 & 0 & 0 \end{bmatrix}. \tag{5}$$

In in the limit of vanishing Reynolds number, Eq. (1) reduces to the well-known results of Schowalter *et al.*[26] and Frankel and Acrivos[30].

The asymptotic expression for the stress in the limit of small inertia for a dilute inertial emulsion in Eq. (1) is an example where the presence of inertia allows for violation of the principle of frame invariance to solid body rotation[23, 37]. In particular, focusing on the last term in Eq. (1), note that the numerical coefficients multiplying the substantial time derivative of $\underline{\underline{\mathrm{D}}}$ and the corrotational terms, $\left(\underline{\underline{\Omega}}\cdot\underline{\underline{\mathrm{D}}}-\underline{\underline{\mathrm{D}}}\cdot\underline{\underline{\Omega}}\right)$, are not the same in the presence of inertia. This can be more clearly understood by comparing the general form of Eq. (1) to the form of the retarded motion expansion[38, 39] developed for flows that vary slowly on the microscale (thus inertialess), truncated at second order (corresponding to a second order fluid), which is given as

$$\frac{\underline{\underline{\sigma}}}{\mu} = 2\underline{\underline{\mathrm{D}}} - \psi_1\left(\frac{D}{Dt}\underline{\underline{\mathrm{D}}} + 2\underline{\underline{\mathrm{D}}}\cdot\underline{\underline{\mathrm{D}}} - \left(\underline{\underline{\Omega}}\cdot\underline{\underline{\mathrm{D}}} - \underline{\underline{\mathrm{D}}}\cdot\underline{\underline{\Omega}}\right)\right) + 4\psi_2\underline{\underline{\mathrm{D}}}\cdot\underline{\underline{\mathrm{D}}}\ . \tag{6}$$

Note that in this expression the same numerical coefficient ψ_1 is multiplying both the substantial time derivative of $\underline{\underline{\mathrm{D}}}$ and the corrotational terms, $\left(\underline{\underline{\Omega}}\cdot\underline{\underline{\mathrm{D}}}-\underline{\underline{\mathrm{D}}}\cdot\underline{\underline{\Omega}}\right)$, as fixed by the requirements of frame invariance to solid body rotation[39] with the expression weighted by ψ_1 simply representing the upper convected derivative of $\underline{\underline{\mathrm{D}}}$, which is duly satisfying the frame invariance principle, hence its presence in most inertialless second order tensor evolution equations[38]. Therefore, it is clear from Eq. (1), as, in general, different coefficients weight the substantial time derivative and the corotational terms for nonzero particle Reynolds number values, that the presence of inertia leads to the violation of material frame invariance. This is however acceptable as this principle has been developed explicitly in the absence of microscopic inertia[37].

The availability of additional results from microscopic simulations[22] provides other, independent, data to validate the resultant inertial emulsion flow model, as will be discussed in subsequent sections. In particular, although the microscopic theory results in Eq. (1) do not provide any information on the orientation and deformation of emulsion droplets, the microscopic simulations quoted can provide both rheological and microstructural information. This allows for direct comparison of all the predictions arising

from the macroscopic emulsion PITCEE model, both on the stress tensor and the droplet orientation and deformation. The following section outlines the development of the PITCEE model through the single generator bracket approach of Non-Equilibrium Thermodynamics (NET).

III. GENERAL DEVELOPMENT OF A PARTICLE INERTIA TCEE (PITCEE) MODEL

The bracket formulation of NET provides a systematic approach to develop macroscopic model equations. For a full account of the assumptions and physical foundation of the single generator bracket formalism the interested reader is referred to the relevant monograph[35]. Here we will highlight its most important to this work characteristics. There are two key elements required to develop macroscopic equations in the single generator bracket approach of NET[35]: (i) a system Hamiltonian, expressing the total energy of the system, that is a function of given state variables and (ii) the Poisson and dissipation brackets, expressing the reversible and irreversible dynamics, respectively. In general, the Poisson bracket is well-known and well-defined once the state variables are decided since their evolution is fully specified by time- reversible, Hamiltonian dynamics in the absence of any dissipation. In contrast, the dissipation bracket is always approximate, requiring modeling of the irreversible dynamics in the system. Its mathematical expression involves phenomenological matrices that express dissipative effects including viscous dissipation, structural relaxation and non-affine effects[35]. Non-equilibrium thermodynamics and continuum mechanics principles (such as the requirement of a local non-negative entropy production rate, the Onsager/Casimir symmetry relations and the principle of material objectivity) can be profitably used to place restrictions on the phenomenological matrices entering the dissipation bracket, but they can never fully determine them. For that task, comparisons against known limiting cases where microscopic modeling results are available and/or against experimental data are needed.

The details of applying the single generator bracket approach of NET towards developing material flow models for dilute emulsions in the limit of inertialess flows have been outlined in Mwasame *et al.*[18]. The most important finding from this work is the demonstration that the availability of microscopic-based asymptotic analysis results in the limit of small Capillary numbers enable not only the validation of the bracket-based macroscopic theory, but also allow the full determination of the model parameters of a minimal model so constructed as to allow those asymptotic results to be quantitatively recovered (the so-called Thermodynamically Consistent Ellipsoidal Emulsion (TCEE) model). However, an important limitation of the TCEE model is that in its development particle inertial effects were neglected a priori. Although this constitutes a common assumption in describing material flow behavior---see, for example,

Bird *et al.*[38] ---as a result of the microscopic size of the material particles, there are situations that frequently arise in applications where either the size of the particles (e.g., through aggregation or coalescence) or the flow intensity increase, or both. Under these circumstances, particle inertia effects can produce non-negligible effects.

An important consideration regarding the bracket approach of NET is that material inertial effects can be easily accommodated. In fact, the reversible component of the dynamics, described by the Poisson bracket, only assumes its natural, canonical, form when both structural and the corresponding momentum variables are included among the state variables. *Rather, it is the inertialess form that is an approximation.* Consequently, one should expect that the macroscopic inertial flow model for dilute emulsions can naturally emerge from the bracket formalism of NET framework once allowance is made to suitably enlarge the state space to accommodate the conformation momentum tensor corresponding to the conformation tensor variable. In this case, the availability of the inertialess TCEE model can be profitably used both as a starting point in the model development and for validation of the final resulting model ensuring consistency to the TCEE model to which it should reduce to in the limit of zero inertia.

The development of the full inertial model for dilute emulsions also benefits from previous developments in the modeling of liquid crystalline systems, which represent the first documented case where micro inertial effects were included in material constitutive equations[33-35]. Moreover, in the last reference by Beris and Edwards[35], the full bracket structures corresponding to three different descriptions of liquid crystals (vector, vector and scalar, and tensor) have been developed and in each one of these three cases for both the full inertial and inertialess approximations. By comparing those two descriptions in all these three cases, the following four main steps are identified in order to obtain the full canonical inertial bracket description: A. an expanded set of variables that enter the state space $\underline{Z}(t,\underline{X})$, B. an extended expression for the free energy, i.e., the Hamiltonian of the system, which is a function of all the system variables, C. an appropriate inertial Poisson bracket to express the reversible dynamics involving the canonical fully antisymmetric coupling between the structural and corresponding momentum variables and D. an appropriate dissipation bracket expressing the irreversible dynamics that in general can involve different phenomenological matrices than the inertialess description. However, the two descriptions are related by the consistency requirement. These four steps are described in more detail below.

A. The expanded state space

There are four variables that enter the state space $\underline{z}(t,\underline{x})$ for a dilute emulsion, one of which (the scalar mass density ρ), is trivially constant in the incompressible flow case considered here and therefore, can be subsequently ignored from the set of relevant state variables of the system. The rest of the variables are: a) two variables that have been used in the inertialess description[18]: the momentum density vector $\underline{u}$, and a contravariant conformation tensor, $\underline{\underline{C}}$, representing by a three-dimensional ellipsoidal the deformed shape of an emulsion droplet, and b) an additional inertial tensor variable, $\underline{\underline{w}}$, that physically describes the corresponding to the conformation tensor structural momentum. The two tensor variables merit additional discussion. The definition of the conformation tensor follows Maffetone & Minale[7]: Its eigenvectors and eigenvalues correspond to the direction and square of the dimensionless magnitude, respectively, of the principal semi-axes of the droplet represented as an ellipsoid. In our previous work[18], we have shown that this definition guarantees that the conformation tensor is physically a contravariant tensor quantity, which therefore automatically fixes its reversible dynamics. Moreover, for convenience, $\underline{\underline{C}}$ is made dimensionless using the radius, R , of the equivalent spherical equilibrium droplet. For a droplet with constant volume $V(t)=V$, the corresponding equilibrium droplet size is defined as $R\equiv\left(V/4\pi\right)^{1/3}$. By neglecting coalescence and breakage as well as diffusive mass transfer processes, e.g., Ostwald ripening, the emulsion droplet volume is preserved, and this constraint is expressed mathematically as

$$I_3\equiv\det\left(\underline{\underline{C}}\right)=1, \tag{7}$$

where I_3 is the third invariant of $\underline{\underline{C}}$. This invariant assumes the value of one when $\underline{\underline{C}}$ is normalized based on the equilibrium spherical droplet dimensions, as is the case here, thus preserving the drop volume[18]. The second tensor variable $\underline{\underline{w}}$ represents, as mentioned, a 'structural momentum' tensor, which is necessary to pair with the conformation tensor to properly represent the canonical dynamics in the material inertial framework and is related to the rate of change in time of the conformation tensor. Thus, for an incompressible system, the relevant state space for the subsequent discussion is $\underline{z}=[\underline{u},\underline{\underline{C}},\underline{\underline{w}}]$.

B. The free energy expression of the system Hamiltonian

The Hamiltonian of a dilute emulsion when considering micro inertia is given by adding an extra, (structural) inertial, term to the previously developed inertialess expression by Mwasame *et al.*[18] as

$$H\left(\underline{\mathrm{u}},\underline{\underline{\mathrm{C}}},\underline{\underline{\mathrm{w}}}\right)=\int\left(\underbrace{\frac{\underline{\underline{\mathrm{u}}}\cdot\underline{\mathrm{u}}}{2\rho}+\phi\Gamma h\left(I_1,I_2\right)+h(T)s(\phi)}_{Inertialess}+\underbrace{\frac{1}{2Z}\underline{\underline{\mathrm{w}}}:\underline{\underline{\mathrm{w}}}}_{Inertial}\right)d\underline{\mathrm{r}}\ , \tag{8}$$

where Z is an inertial parameter, entering the canonical description of the (structurally) inertial kinetic energy (last term in the right-hand-side of Eq. (8)) in an analogous fashion to the mass density ρ entering the description of standard (momentum) kinetic energy (first term in the right-hand-side of Eq. (8)). As the physical interpretation of the inertial parameter Z cannot be specified a-priori, its significance will be discussed in Section IV with respect to comparison against existing asymptotic theory. The second and third terms appearing in the right-hand-side of Eq. (8) are modeling the surface energy of the droplets and the mixing entropy, respectively. The parameters in the above expression are defined as follows: Γ is the surface energy density defined as the ratio of the surface tension (γ) and the radius of the droplet (R), h is the dimensionless surface area of the ellipsoidal droplet normalized by the equilibrium un-deformed surface area, ϕ is the volume fraction of the droplets, k_B is the Boltzmann's constant and $s(\phi)$ is the entropy density. In addition, there is an equilibrium contribution to the Hamiltonian expression mentioned above, which however, as only a function of temperature and pressure, is unimportant for the following analysis.

The dimensionless surface area h for a deformed ellipsoid is approximated using Knud Thomsen's formula[40] in terms of the eigenvalues of $\underline{\underline{\mathrm{C}}}$ (which themselves can be expressed equivalently in terms of the invariants $\left(I_1,I_2\right)$ of $\underline{\underline{\mathrm{C}}}$) as

$$h=\frac{S_D}{4\pi R^2}=\left(\frac{\lambda_1^{\omega/2}\lambda_2^{\omega/2}+\lambda_2^{\omega/2}\lambda_3^{\omega/2}+\lambda_3^{\omega/2}\lambda_1^{\omega/2}}{3}\right)^{\frac{1}{\omega}}\ ;\ \omega=8/5\ . \tag{9}$$

In the expression above, S_D is the dimensional surface area of the deformed droplet and λ_1, λ_2 and λ_3 are eigenvalues of $\underline{\underline{\mathrm{C}}}$. The use of the Knud Thomsen's formula to express the surface area of an ellipsoid has been previously justified[18], where it was also shown that this expression is especially accurate at small deformations of the droplets from sphericity.

C. The inertial Poisson and Dissipative brackets in the single generator approach

The starting point of the single generator bracket description of NET is that the time evolution for any arbitrary functional F of the N-dimensional state space, $\underline{Z}(t,\underline{x})$, is generated by a linear superposition of the Poisson $\{\square,\square\}$ and Dissipative $[\square,\square]$ brackets as (Beris & Edwards 1994)

$$\frac{dF}{dt}=\{F,H\}+[F,H]\equiv\int_{\Omega}\sum_{k=1}^{N}\frac{\delta F}{\delta z_k}\frac{\partial z_k}{\partial t}d\Omega. \tag{10}$$

These two brackets dictate the reversible and irreversible dynamics, respectively. The brackets are functionals of F and H and they obey specific symmetry/antisymmetry properties[35] with H representing the Hamiltonian (extended free energy) of the system provided here by Eqs. (8) and (9). In Eq. (10), the second equality is derived following the standard chain rule of differentiation and provides the connection between the evolution equations for the system variables and the structure of the brackets. In the same expression, Ω denotes the bulk volume phase space

The Poisson bracket consists solely of antisymmetric terms that therefore do not contribute to entropy generation (i.e., $\{H,H\}=0$). The starting point to develop the inertial Poisson bracket for emulsions is the corresponding standard inertialess unconstrained bracket expression for an unconstrained conformation tensor variable $q_{\alpha\beta}$ which is provided by[35]

$$\begin{aligned}\{F,H\}=&-\int\left[\frac{\delta F}{\delta u_\gamma}\nabla_\beta\left(\frac{\delta H}{\delta u_\beta}u_\gamma\right)-\frac{\delta H}{\delta u_\gamma}\nabla_\beta\left(\frac{\delta F}{\delta u_\beta}u_\gamma\right)\right]d^3r\\&-\int\left[\frac{\delta F}{\delta\rho}\nabla_\beta\left(\frac{\delta H}{\delta u_\beta}\rho\right)-\frac{\delta H}{\delta\rho}\nabla_\beta\left(\frac{\delta F}{\delta u_\beta}\rho\right)\right]d^3r\\&-\int\left[\frac{\delta F}{\delta q_{\alpha\beta}}\frac{\delta H}{\delta u_\gamma}\nabla_\gamma q_{\alpha\beta}-\frac{\delta H}{\delta q_{\alpha\beta}}\frac{\delta F}{\delta u_\gamma}\nabla_\gamma q_{\alpha\beta}\right]d^3r\\&-\int q_{\alpha\gamma}\left[\frac{\delta H}{\delta q_{\alpha\beta}}\nabla_\gamma\left(\frac{\delta F}{\delta u_\beta}\right)-\frac{\delta F}{\delta q_{\alpha\beta}}\nabla_\gamma\left(\frac{\delta H}{\delta u_\beta}\right)\right]d^3r\\&-\int q_{\beta\gamma}\left[\frac{\delta H}{\delta q_{\alpha\beta}}\nabla_\gamma\left(\frac{\delta F}{\delta u_\alpha}\right)-\frac{\delta F}{\delta q_{\alpha\beta}}\nabla_\gamma\left(\frac{\delta H}{\delta u_\alpha}\right)\right]d^3r\end{aligned}. \tag{11}$$

Note that here and in the following, Einstein's implicit summation convention for any pair of repeated subscript indices is followed with the repeated indices taking values between 1 and 3. The Poisson bracket above expresses the reversible dynamics of the state variables ρ, μ_α and an unconstrained conformation variable $q_{\alpha\beta}$, and the physical implications of the various terms will be discussed shortly.

To add inertial effects into the resultant unconstrained bracket equations above requires specifying additional terms in the Poisson bracket that express the coupling between the structural momentum variable $w_{\alpha\beta}$ and the momentum density u_α, as well as the coupling between $w_{\alpha\beta}$ and the conformation tensor $q_{\alpha\beta}$ respectively. These additional contributions to the Poisson bracket above, denoted $\{F,H\}_{extra}$, have already been derived with regards to inertial models for liquid crystalline systems[35] and are given by

$$\begin{aligned}\{F,H\}_{extra} &= -\int\left[\frac{\delta F}{\delta w_{\alpha\beta}}\frac{\delta H}{\delta q_{\alpha\beta}} - \frac{\delta H}{\delta w_{\alpha\beta}}\frac{\delta F}{\delta q_{\alpha\beta}}\right]d^3r \\ &-\int\left[\frac{\delta F}{\delta w_{\alpha\beta}}\nabla_\gamma\left(\frac{\delta H}{\delta u_\gamma}w_{\alpha\beta}\right) - \frac{\delta H}{\delta w_{\alpha\beta}}\nabla_\gamma\left(\frac{\delta F}{\delta u_\gamma}w_{\alpha\beta}\right)\right]d^3r\end{aligned} \tag{12}$$

The above expressions in Eqs. (11) and (12) do not enforce a unit determinant constraint on the conformation variable $q_{\alpha\beta}$. The corresponding inertial Poisson bracket that enforces a unit determinant constraint can be derived from Eqs. (11) and (12) by first making the identification

$$\underline{\underline{q}} \rightarrow \underline{\underline{C}} = \frac{\underline{\underline{q}}}{\left(\det\left(\underline{\underline{q}}\right)\right)^{1/3}} \ . \tag{13}$$

Through this relationship, the Volterra derivatives with respect to the $q_{\alpha\beta}$ tensor can be expressed in terms of the determinant constrained variable $C_{\alpha\beta}$ as

$$\frac{\delta F}{\delta q_{\alpha\beta}} = \frac{\delta F}{\delta C_{\gamma\varepsilon}}\frac{\delta C_{\gamma\varepsilon}}{\delta q_{\alpha\beta}} = \frac{\delta F}{\delta C_{\gamma\varepsilon}}\left(\delta_{\alpha\gamma}\delta_{\beta\varepsilon} - \frac{1}{3}C_{\gamma\varepsilon}C^{-1}_{\alpha\beta}\right) \ . \tag{14}$$

Substituting this expression, also provided by Eq. (21) in Edwards et al.[41], into Eq. (11) alone yields the constrained inertialess brackets (for a unit determinant) that appear in the TCEE model[18]. Including the expression into Eqs. (11) and (12) leads to the final inertial constrained Poisson bracket equation for the $C_{\alpha\beta}$ tensor which is given by

$$
\begin{aligned}
\{F,H\} = &-\int\left[\frac{\delta F}{\delta u_\gamma}\nabla_\beta\left(\frac{\delta H}{\delta u_\beta}u_\gamma\right)-\frac{\delta H}{\delta u_\gamma}\nabla_\beta\left(\frac{\delta F}{\delta u_\beta}u_\gamma\right)\right]d^3r \\
&-\int\left[\frac{\delta F}{\delta \rho}\nabla_\beta\left(\frac{\delta H}{\delta u_\beta}\rho\right)-\frac{\delta H}{\delta \rho}\nabla_\beta\left(\frac{\delta F}{\delta u_\beta}\rho\right)\right]d^3r \\
&-\int\left[\frac{\delta F}{\delta C_{\alpha\beta}}\frac{\delta H}{\delta u_\gamma}\nabla_\gamma C_{\alpha\beta}-\frac{\delta H}{\delta C_{\alpha\beta}}\frac{\delta F}{\delta u_\gamma}\nabla_\gamma C_{\alpha\beta}\right]d^3r \\
&+\frac{1}{3}\int C_{\alpha\beta}\left[\frac{\delta H}{\delta C_{\alpha\beta}}C^{-1}_{\rho\eta}\left(\frac{\delta F}{\delta u_\gamma}\right)\nabla_\gamma C_{\rho\eta}-\frac{\delta F}{\delta C_{\alpha\beta}}C^{-1}_{\rho\eta}\left(\frac{\delta H}{\delta u_\gamma}\right)\nabla_\gamma C_{\rho\eta}\right]d^3r \\
&-\int C_{\alpha\gamma}\left[\frac{\delta H}{\delta C_{\alpha\beta}}\nabla_\gamma\left(\frac{\delta F}{\delta u_\beta}\right)-\frac{\delta F}{\delta C_{\alpha\beta}}\nabla_\gamma\left(\frac{\delta H}{\delta u_\beta}\right)\right]d^3r \\
&-\int C_{\beta\gamma}\left[\frac{\delta H}{\delta C_{\alpha\beta}}\nabla_\gamma\left(\frac{\delta F}{\delta u_\alpha}\right)-\frac{\delta F}{\delta C_{\alpha\beta}}\nabla_\gamma\left(\frac{\delta H}{\delta u_\alpha}\right)\right]d^3r \\
&+\frac{2}{3}\int C_{\alpha\beta}\left[\frac{\delta F}{\delta C_{\alpha\beta}}\nabla_\gamma\left(\frac{\delta H}{\delta u_\gamma}\right)-\frac{\delta H}{\delta C_{\alpha\beta}}\nabla_\gamma\left(\frac{\delta F}{\delta u_\gamma}\right)\right]d^3r \\
&-\int\left[\frac{\delta F}{\delta w_{\alpha\beta}}\frac{\delta H}{\delta C_{\alpha\beta}}-\frac{\delta H}{\delta w_{\alpha\beta}}\frac{\delta F}{\delta C_{\alpha\beta}}\right]d^3r \\
&-\frac{1}{3}\int C_{\rho\eta}\left[\frac{\delta H}{\delta w_{\alpha\beta}}C^{-1}_{\alpha\beta}\frac{\delta F}{\delta C_{\rho\eta}}-\frac{\delta F}{\delta w_{\alpha\beta}}C^{-1}_{\alpha\beta}\frac{\delta H}{\delta C_{\rho\eta}}\right]d^3r \\
&-\int\left[\frac{\delta F}{\delta w_{\alpha\beta}}\nabla_\gamma\left(\frac{\delta H}{\delta u_\gamma}w_{\alpha\beta}\right)-\frac{\delta H}{\delta w_{\alpha\beta}}\nabla_\gamma\left(\frac{\delta F}{\delta u_\gamma}w_{\alpha\beta}\right)\right]d^3r
\end{aligned}
\quad . \qquad (15)
$$

In the above expression, the first term provides the reversible dynamics of the momentum density variable, the second term provides the dynamics of the mass density that leads to the continuity equation, which is unimportant for incompressible systems in which mass is conserved. The third, to seventh term lead to the standard upper-convected time derivative that governs the dynamics of any contravariant second order tensor, such as the conformation tensor, plus some additional correcting terms emerging from the unit determinant constraint---see Mwasame *et al.*[18] for further details. The eighth and ninth terms account for the (canonical) dynamic coupling between the inertial and conformational tensor variables including the necessary correction emerging from the unit determinant constraint. The remaining terms account for the standard reversible dynamics of the inertial variable tensor $\underline{\underline{w}}$. Note

that the first seven lines in Eq. (15) express exactly the Poisson bracket determined in the inertialess limit[18].

There is no simple transformation through which the dissipation bracket can be similarly derived from its inertialess counterpart. Instead, the correct structure of the dissipation bracket is judged by ensuring that the final inertial model equations can reduce to the corresponding inertialess TCEE model equations in the appropriate limit. Following this requirement, the inertial dissipation bracket is established following standard NET practices as a general bilinear form coupling the various Volterra derivatives[35] according to the rules of continuum mechanics as

$$\begin{aligned}\left[F,H\right]_{wec} \equiv -\int R_{\alpha\beta\gamma\varepsilon}
\begin{pmatrix}
\left(\begin{array}{c}\dfrac{\delta F}{\delta w_{\alpha\beta}}+\dfrac{\xi}{2}C_{\alpha\eta}\left(\nabla_\eta\dfrac{\delta F}{\delta u_\beta}+\nabla_\beta\dfrac{\delta F}{\delta u_\eta}\right)+\dfrac{\xi}{2}C_{\beta\eta}\left(\nabla_\eta\dfrac{\delta F}{\delta u_\alpha}+\nabla_\alpha\dfrac{\delta F}{\delta u_\eta}\right)\\ -\dfrac{\zeta}{2}C_{\alpha\eta}\left(\nabla_\eta\dfrac{\delta F}{\delta u_\beta}-\nabla_\beta\dfrac{\delta F}{\delta u_\eta}\right)+\dfrac{\zeta}{2}C_{\beta\eta}\left(\nabla_\eta\dfrac{\delta F}{\delta u_\alpha}-\nabla_\alpha\dfrac{\delta F}{\delta u_\eta}\right)\end{array}\right)\times\\
\left(\begin{array}{c}\dfrac{\delta H}{\delta w_{\gamma\varepsilon}}+\dfrac{\xi}{2}C_{\gamma\eta}\left(\nabla_\eta\dfrac{\delta H}{\delta u_\varepsilon}+\nabla_\varepsilon\dfrac{\delta H}{\delta u_\eta}\right)+\dfrac{\xi}{2}C_{\varepsilon\eta}\left(\nabla_\eta\dfrac{\delta H}{\delta u_\gamma}+\nabla_\gamma\dfrac{\delta H}{\delta u_\eta}\right)\\ -\dfrac{\zeta}{2}C_{\gamma\eta}\left(\nabla_\eta\dfrac{\delta H}{\delta u_\varepsilon}-\nabla_\varepsilon\dfrac{\delta H}{\delta u_\eta}\right)+\dfrac{\zeta}{2}C_{\varepsilon\eta}\left(\nabla_\eta\dfrac{\delta H}{\delta u_\gamma}-\nabla_\gamma\dfrac{\delta H}{\delta u_\eta}\right)\end{array}\right)
\end{pmatrix} d^3r\\
-\int Q_{\alpha\beta\gamma\varepsilon}\left(\nabla_\alpha\frac{\delta F}{\delta u_\beta}\right)\left(\nabla_\gamma\frac{\delta H}{\delta u_\varepsilon}\right)d^3r\end{aligned}$$

(16)

The subscript wec means "without entropy production correction", i.e., without terms involving derivatives with respect to entropy, which are unimportant when describing (as here) the dynamics of isothermal systems. $R_{\alpha\beta\gamma\varepsilon}$ and $Q_{\alpha\beta\gamma\varepsilon}$ are defined as positive definite phenomenological fourth order tensors to ensure thermodynamically admissibility of the model. These tensors represent the relaxation and viscous dissipation effects, respectively, following the general arguments described in ref. 35. These phenomenological tensors have units of time and pascal-seconds respectively and are symmetric with respect to the following interchanges of indices: $\alpha\leftrightarrow\beta,\gamma\leftrightarrow\varepsilon$ and $\left(\alpha,\beta\right)\leftrightarrow\left(\gamma,\varepsilon\right)$, following the standard Onsager/Casimir symmetry relations[35]. Finally, ξ and ζ are non-affine parameters whose physical interpretation will be discussed shortly.

A few words of explanation regarding the proposed form of the dissipation bracket are warranted here. First, the last term, representing standard viscous effects, reproduces here exactly a similar term appearing in the inertialess dissipation bracket[18]. Second, as the first term one would initially have proposed a much simpler bilinear symmetric expression involving just that Volterra derivative with respect to the (structural) inertial variable $\underline{\underline{w}}$ as $-\int R_{\alpha\beta\gamma\varepsilon}\frac{\delta F}{\delta w_{\alpha\beta}}\frac{\delta H}{\delta w_{\gamma\varepsilon}}\ d^3r$. However, such a term alone could not have accounted for the antisymmetric dissipation term coupling the Volterra derivative with respect the conformation tensor and the gradient of the Volterra derivative with respect to the momentum density that appeared in the inertialess formalism[18]. Note that even for the case of the liquid crystals, similar terms accompanying the Volterra derivatives of the structural momentum tensor appear in the corresponding dissipative brackets[35]. Furthermore, we note that during the transition from the inertialess approximation to the inertial dissipation bracket, when we replace Volterra derivative of the conformation tensor (a quantity of even parity upon time reversal) with the Volterra derivative of the structural momentum tensor (a quantity with odd parity upon time reversal), the corresponding coupling to the gradient of the Volterra derivative with respect to the momentum density (a quantity with odd parity upon time reversal) must also change from antisymmetric to symmetric, respectively. Such couplings should be included as representing the cross terms of the most general bilinear form involving the Volterra derivatives with respect to either the conformation or structural momentum tensor from the one hand (in the inertialess or inertial descriptions, respectively) and the gradient of the Volterra derivative with respect to the momentum density, from the other.

What is really new though in the expression proposed in Eq. (16) for the inertial dissipation bracket is that, as this expression applies for the case of an inertial model, the cross terms involve more than the symmetric part of the gradient of the Volterra derivative with respect to the momentum density. It is noteworthy that the symmetric contribution, weighted by the non-affine parameter ξ, eventually ends up modifying the upper-convected derivative when we evaluate the resulting evolution equation for the conformation tensor to give rise to the Gordon-Schowalter derivative. More importantly, the new coupling in Eq. (16) involves an additional non-affine parameter ζ that weights the antisymmetric part of the gradient of the Volterra derivative with respect to the momentum density. This term introduces additional correction terms to the upper-convected time derivative that further modify the Gordon-Schowalter derivative to include a term proportional to the flow vorticity. This new term also makes the final evolution equation non-objective. However, as the resulting material model is inertial in origin, we

cannot apply any objectivity criterion to the corresponding equations with respect to arbitrary moving coordinate frames. Rather, equation invariance is limited to only with respect to Galilean frames, i.e., those which correspond, at most, to a steady uniform translation of one with respect to the other. Physically, the scalar parameter ξ weights non-affine effects arising from the mismatch in the deformation between a partially rigid microstructure (e.g., polymer chain or emulsion droplet) and the surrounding matrix fluid. On the other hand, the new non-affine scalar parameter ζ represents the lowest order micro-inertia correction, which affects the relative rotation, as will be justified in the following.

The inertial dissipative bracket in Eq. (16) has a number of novel features compared to related inertial theory previously discussed with regards to liquid crystalline polymers[35] and consequently, substantially corrects the inertial theory for emulsions proposed by Dressler[36]. In particular, all dissipative effects that involve the conformation tensor are mediated through a single fourth order tensor, $R_{\alpha\beta\gamma\varepsilon}$, combining the roles of both the relaxation tensor $\Lambda_{\alpha\beta\gamma\varepsilon}$ and the non-affine coupling tensor $L_{\alpha\beta\gamma\varepsilon}$ appearing in the inertialess approximation[18]. This is to be contrasted against the inertial liquid crystal polymer models, where we not only have a very particular case corresponding to $R_{\alpha\beta\gamma\varepsilon}=\frac{1}{2}\left(\delta_{\alpha\gamma}\delta_{\beta\varepsilon}+\delta_{\alpha\varepsilon}\delta_{\beta\gamma}\right)$, but the effects of the non-affine motion are combined with those from the upper-convected terms of the upper-convected derivative resulting in the dissipative terms splitting into two: one weighted by $\left(1-\xi\right)/2$ and the other by $\left(1+\xi\right)/2$. Also, there is no equivalent ζ-weighted term coupling the conformation tensor to the vorticity. These differences are explained by the different physics described in these two situations; the emulsion case describes flow-deformation effects, while the liquid crystalline case describes the effects of rigid body rotation[35]. An additional check that the inertial brackets presented in Eqs. (15) and (16) are the correct ones will be presented once the resultant macroscopic equations (i.e., those representing the PITCEE model) are developed from the inertial brackets through the direct comparison of the predictions resulting from the PITCEE model against available microscopically-based asymptotic results---see Section IV below. However, before deriving the PITCEE model equations, one needs first to properly identify the Volterra derivatives of the Hamiltonian as described in the next section.

D. The Volterra derivatives of the Hamiltonian

The Volterra derivative of the Hamiltonian with respect to the conformation tensor in the presence of a unit determinant constraint must be defined such that it is always constrained to the appropriate subspace and its proper derivation has been discussed in detail[18]. For completion purposes the final expression is also reproduced here:

$$\frac{\delta H}{\delta C_{\gamma\varepsilon}} = \phi\Gamma\left(\left(\partial h/\partial I_1\right)\left(\delta_{\gamma\varepsilon} - \left(\frac{I_2}{I_2^2 - 2I_1} \right) C^{-1}_{\gamma\varepsilon} \right) + \left(\partial h/\partial I_2\right)\left(I_1\delta_{\gamma\varepsilon} - C_{\gamma\varepsilon} - \left(\frac{I_1 I_2 - 3}{I_2^2 - 2I_1} \right) C^{-1}_{\gamma\varepsilon} \right) \right), \quad (17)$$

where I_1 and I_2 are the first and second invariants of the conformation tensor respectively defined as

$$I_1 \equiv \mathrm{tr}\left(\underline{\underline{\mathrm{C}}}\right) = \lambda_1 + \lambda_2 + \lambda_3 \ , \quad (18)$$

and

$$I_2 \equiv \frac{1}{2}\left(\left(\mathrm{tr}\left(\underline{\underline{\mathrm{C}}}\right)\right)^2 - \mathrm{tr}\left(\underline{\underline{\mathrm{C}}} \cdot \underline{\underline{\mathrm{C}}}\right) \right) = \lambda_1\lambda_2 + \lambda_2\lambda_3 + \lambda_1\lambda_3 , \quad (19)$$

where the λ_i's are the eigenvalues of $\underline{\underline{\mathrm{C}}}$. In these expressions, tr( ) is defined as the trace. The partial derivatives $\partial h/\partial I_1$ and $\partial h/\partial I_2$ that appear in Eq. (17) are obtained through the use of the Knud Thomsen's formula[40] given by Eq. (9), are given as

$$\partial h/\partial I_1 = \frac{3^{-\frac{1}{\omega}}\left(\lambda_1^{\omega/2}\lambda_2^{\omega/2} + \lambda_2^{\omega/2}\lambda_3^{\omega/2} + \lambda_3^{\omega/2}\lambda_1^{\omega/2}\right)^{\frac{1}{\omega}-1}}{2\left(\lambda_1^2\lambda_2 - \lambda_1\lambda_2^2 - \lambda_1^2\lambda_3 + \lambda_2^2\lambda_3 + \lambda_1\lambda_3^2 - \lambda_2\lambda_3^2\right)} \times \left(\left(\lambda_1\lambda_2\right)^{\frac{\omega}{2}-1}\left(\lambda_2 - \lambda_1\right) + \left(\lambda_2\lambda_3\right)^{\frac{\omega}{2}-1}\left(\lambda_3 - \lambda_2\right) + \left(\lambda_1\lambda_3\right)^{\frac{\omega}{2}-1}\left(\lambda_1 - \lambda_3\right) \right) , \quad (20)$$

and

$$\partial h/\partial I_2 = \frac{3^{-\frac{1}{\omega}}\left(\lambda_1^{\omega/2}\lambda_2^{\omega/2} + \lambda_2^{\omega/2}\lambda_3^{\omega/2} + \lambda_3^{\omega/2}\lambda_1^{\omega/2}\right)^{\frac{1}{\omega}-1}}{2\left(\lambda_1^2\lambda_2 - \lambda_1\lambda_2^2 - \lambda_1^2\lambda_3 + \lambda_2^2\lambda_3 + \lambda_1\lambda_3^2 - \lambda_2\lambda_3^2\right)} \times \left(\left(\lambda_1\lambda_2\right)^{\frac{\omega}{2}}\left(\lambda_1 - \lambda_2\right) + \left(\lambda_2\lambda_3\right)^{\frac{\omega}{2}}\left(\lambda_2 - \lambda_3\right) + \left(\lambda_1\lambda_3\right)^{\frac{\omega}{2}}\left(\lambda_3 - \lambda_1\right) \right) , \quad (21)$$

respectively, where the value of $\omega = 8/5$. Note that the subscript differentiates the eigenvalue notation from that of the viscosity ratio which is simply denoted λ -see for example Eq. (1).

The Volterra derivative of the Hamiltonian with respect to $w_{\alpha\beta}$, as computed from the extended free energy expression provided in Eq. (8), is given as

$$\frac{\delta H}{\delta w_{\alpha\beta}} = \frac{w_{\alpha\beta}}{Z} \equiv \overline{w}_{\alpha\beta} \ . \tag{22}$$

Finally, the Volterra derivative with respect to the momentum density is evaluated as usual as

$$\frac{\delta H}{\delta u_{\alpha}} = \frac{u_{\alpha}}{\rho} = v_{\alpha} \ , \tag{23}$$

where v_{α} represents the velocity field.

E. PITCEE model equations

The governing evolution equations of the field variables in the PITCEE model are determined, as usual[35], by forcing Eq. (10) for an arbitrary functional *F* of $\underline{z} = [\underline{u}, \underline{\underline{C}}, \underline{\underline{w}}]$ using the brackets defined in Eqs. (15) and (16). This results first in the following evolution equation for the rescaled structural momentum tensor $\underline{\underline{\overline{w}}}$, defined in Eq. (22), as

$$Z\frac{D\overline{w}_{\alpha\beta}}{Dt} = -\frac{\delta H}{\delta C_{\alpha\beta}} + \frac{1}{3}C^{-1}_{\alpha\beta}C_{\rho\eta}\frac{\delta H}{\delta C_{\rho\eta}} - R_{\alpha\beta\gamma\varepsilon}\left(\frac{\delta H}{\delta w_{\gamma\varepsilon}} + \xi\left(C_{\gamma\eta}D_{\eta\varepsilon} + D_{\gamma\eta}C_{\eta\varepsilon}\right) + \zeta\left(\Omega_{\gamma\eta}C_{\eta\varepsilon} - C_{\gamma\eta}\Omega_{\eta\varepsilon}\right)\right)$$

,(24)

where $\overset{\nabla}{\bullet}$ represents the upper-convected derivative. Second, the evolution equation for the conformation tensor, $\underline{\underline{C}}$, is provided (after simplifications due to incompressibility) by

$$\overset{\nabla}{C}_{\alpha\beta} + \frac{1}{3}C_{\alpha\beta}C^{-1}_{\rho\eta}v_{\gamma}\nabla_{\gamma}C_{\rho\eta} = \overline{w}_{\alpha\beta} - \frac{1}{3}C_{\alpha\beta}C^{-1}_{\rho\eta}\overline{w}_{\rho\eta} \ . \tag{25}$$

Finally, the extra stress tensor is extracted from the evolution equation for the momentum density variable, $\underline{u}$, as

$$\sigma_{\alpha\beta} = Q_{\alpha\beta\gamma\varepsilon}\nabla_{\gamma}v_{\varepsilon} + 2(1-\xi)\left(C_{\beta\gamma}\frac{\delta H}{\delta C_{\alpha\gamma}} - \frac{1}{3}C_{\rho\eta}\frac{\delta H}{\delta C_{\rho\eta}}\delta_{\alpha\beta}\right) - 2\xi C_{\beta\gamma}Z\frac{D\overline{w}_{\alpha\gamma}}{Dt} \ . \tag{26}$$

These equations complete the PITCEE model. Note that in developing these equations, a unit determinant constraint on $\underline{\underline{C}}$ is enforced following the rules developed by Mwasame *et al.*[18] following the guidelines

established by Edwards *et al*.[41]. In the following section, we demonstrate how the PITCEE model parameters may be determined.

F. Specification of the phenomenological matrices

The expressions provided by Eqs. (24)-(26) represent the inertial model equations. Further progress requires specification of $R_{\alpha\beta\gamma\varepsilon}$, the relaxation matrix. One method to identify $R_{\alpha\beta\gamma\varepsilon}$ is to apply Eqs. (24)-(26) in the inertialess limit, obtained by setting both Z and ζ inertial parameters to zero and then by forcing the consistency of the resulting equations to their inertialess counterparts which have been previously derived[18]. Evaluating Eq. (24) for $Z=\zeta=0$ and then taking the double inner product of the resulting equation by $\underset{\equiv\equiv}{\mathrm{R}}^{-1}$, enables solving for $\dfrac{\delta H}{\delta w_{\alpha\beta}}=\bar{w}_{\alpha\beta}$, which when substituting in Eq. (25) gives (taking also into account incompressibility)

$$\overset{\nabla}{C}_{\alpha\beta}+\frac{1}{3}C_{\alpha\beta}C^{-1}_{\rho\eta}v_\gamma\nabla_\gamma C_{\rho\eta}+\xi\left(D_{\alpha\eta}C_{\eta\beta}+C_{\alpha\eta}D_{\eta\beta}\right)=-R^{-1}_{\alpha\beta\gamma\varepsilon}\left(\frac{\delta H}{\delta C_{\gamma\varepsilon}}-\frac{1}{3}C^{-1}_{\gamma\varepsilon}C_{\rho\eta}\frac{\delta H}{\delta C_{\rho\eta}}\right)$$
$$+\frac{1}{3}C_{\alpha\beta}C^{-1}_{\rho\eta}\left(R^{-1}_{\rho\eta\gamma\varepsilon}\left(\frac{\delta H}{\delta C_{\gamma\varepsilon}}-\frac{1}{3}C^{-1}_{\gamma\varepsilon}C_{\kappa\lambda}\frac{\delta H}{\delta C_{\kappa\lambda}}\right)\right) \quad (27)$$

Similarly, applying the same limiting values $Z=\zeta=0$ to Eq. (26) gives

$$\sigma_{\alpha\beta}=Q_{\alpha\beta\gamma\varepsilon}\nabla_\gamma v_\varepsilon+2\left(1-\xi\right)\left(C_{\beta\gamma}\frac{\delta H}{\delta C_{\alpha\gamma}}-\frac{1}{3}C_{\rho\eta}\frac{\delta H}{\delta C_{\rho\eta}}\delta_{\alpha\beta}\right). \quad (28)$$

These equations have exactly the same form as the inertialess TCEE model developed by Mwasame *et al.*[18], Eqs. (29) and (31) in that work. To obtain the identical final equations in the inertialess limit, the following choices need to be made for the phenomenological matrices, taking also into account the form of the corresponding matrices in the inertialess case as given by[18]:

$$R^{-1}_{\alpha\beta\gamma\varepsilon}=\Lambda_{\alpha\beta\gamma\varepsilon}=\frac{3}{4I_2\tau_C\phi\Gamma}\begin{pmatrix}a_2\left(C_{\alpha\gamma}\delta_{\beta\varepsilon}+C_{\alpha\varepsilon}\delta_{\beta\gamma}+C_{\beta\gamma}\delta_{\alpha\varepsilon}+C_{\beta\varepsilon}\delta_{\alpha\gamma}\right)+\\ a_3\left(2C_{\alpha\gamma}C_{\beta\varepsilon}+2C_{\alpha\varepsilon}C_{\beta\gamma}\right)\end{pmatrix}, \quad (29)$$

$$Q_{\alpha\beta\gamma\varepsilon}=\mu\left(1+\phi P(\lambda)\right)\left(\delta_{\alpha\gamma}\delta_{\beta\varepsilon}+\delta_{\beta\gamma}\delta_{\alpha\varepsilon}\right). \quad (30)$$

In the above expressions, τ_C is the Capillary relaxation time defined as $\tau_C\equiv\mu R/\gamma$ such that $\tau_C=Ca^*$ as defined in Eq. (1). In addition, a_2 and a_3 are parameters that weight the relaxation terms while $P(\lambda)$

is a function of the viscosity ratio, λ, of the disperse and continuous phases. The parameters appearing in Eqs. (29) and (30) have been previously evaluated through comparison against relevant asymptotic theory for dilute emulsion rheology in the limit of $Ca \to 0$ and zero Reynolds number[18], as

$$\xi = \frac{2\lambda - 2}{2\lambda + 3}, \tag{31}$$

$$a_2 = \left(\frac{36\left(25\lambda^2 + 41\lambda + 4\right)}{35\left(19\lambda + 16\right)^2} \right)$$
$$a_3 = \left(\frac{300\left(\lambda + 1\right)}{\left(19\lambda + 16\right)\left(2\lambda + 3\right)} - \frac{36\left(25\lambda^2 + 41\lambda + 4\right)}{35\left(19\lambda + 16\right)^2} \right), \tag{32}$$

and

$$P(\lambda) = \frac{\left(5\lambda + 2\right)}{2\left(\lambda + 1\right)} \left(1 - \frac{\left(19\lambda + 16\right)}{\left(5\lambda + 2\right)\left(2\lambda + 3\right)} \right). \tag{33}$$

The specification of the two additional remaining parameters Z and ζ that arise in the inertial formulation of the emulsion model is discussed in the next section.

IV. Determining the inertial model parameters using asymptotic results for small Re_p

To specify the remaining two model parameters, Z and ζ, in the inertial, PITCEE model we proceed, in an analogous fashion to that followed for the determination of the model parameters in the inertialess TCEE model, i.e., by matching the asymptotic expansion of the solution to Eqs. (24)-(26) to asymptotic literature results summarized in Eq. (1), applicable for dilute emulsions with droplet morphology. However, this time we also allow for (small) inertia effects to be present. For convenience, Eqs. (24)-(26) can be re-written using the following scaling relationships:

$$\begin{aligned} \hat{Z} &= Z \Big/ \left(\phi \Gamma Ca^{*2} \right) \\ \frac{\delta \hat{H}}{\delta C_{\alpha\beta}} &= \frac{\delta H}{\delta C_{\alpha\beta}} \Big/ \left(\phi \Gamma^* \right) \\ \hat{R}^{-1}_{\alpha\beta\gamma\varepsilon} &= \hat{\Lambda}_{\alpha\beta\gamma\varepsilon} = \Lambda_{\alpha\beta\gamma\varepsilon} \phi \Gamma Ca^* \end{aligned} . \tag{34}$$

Consequently, Eqs. (24)-(26) can be re-written as

$$\hat{\Lambda}_{\alpha\beta\gamma\varepsilon}\left(\hat{Z}Ca^{*2}\frac{D\overline{w}_{\alpha\beta}}{Dt}+\frac{\delta\hat{H}}{\delta C_{\alpha\beta}}-\frac{1}{3}C^{-1}_{\alpha\beta}C_{\rho\eta}\frac{\delta\hat{H}}{\delta C_{\rho\eta}}\right)= \\ -Ca^{*}\left(\overline{w}_{\alpha\beta}+\xi\left(C_{\gamma\eta}D_{\eta\varepsilon}+D_{\gamma\eta}C_{\eta\varepsilon}\right)+\zeta\left(\Omega_{\gamma\eta}C_{\eta\varepsilon}-C_{\gamma\eta}\Omega_{\eta\varepsilon}\right)\right) \quad , \tag{35}$$

$$\overset{\nabla}{C}_{\alpha\beta}+\frac{1}{3}C_{\alpha\beta}C^{-1}_{\rho\eta}v_{\gamma}\nabla_{\gamma}C_{\rho\eta}=\overline{w}_{\alpha\beta}-\frac{1}{3}C_{\alpha\beta}C^{-1}_{\rho\eta}\overline{w}_{\rho\eta}\,, \tag{36}$$

and

$$\sigma_{\alpha\beta}=Q_{\alpha\beta\gamma\varepsilon}\nabla_{\gamma}v_{\varepsilon}+2\phi\Gamma\left(1-\xi\right)\left(C_{\beta\gamma}\frac{\delta\hat{H}}{\delta C_{\alpha\gamma}}-\frac{1}{3}C_{\rho\eta}\frac{\delta\hat{H}}{\delta C_{\rho\eta}}\delta_{\alpha\beta}\right)-2\xi C_{\beta\gamma}\hat{Z}\phi\Gamma Ca^{*2}\frac{D\overline{w}_{\alpha\gamma}}{Dt}\,. \tag{37}$$

Note that Eq. (35) consists of only dimensionless parameters while Eq (37) is dimensional expressed in pressure units.

Identifying the inertial parameters begins with analyzing the full inertial stress expression in Eq. (37) in a form similar to Eq. (1) as

$$\sigma_{\alpha\beta}=\sigma_{\alpha\beta,00}+\tau_{C}\sigma_{\alpha\beta,01}+\tau_{C}^{2}\sigma_{\alpha\beta,02}+O(\tau_{C}^{3})\,, \tag{38}$$

through an expansion in terms of the Capillary relaxation time $\tau_{C}\equiv\mu_{s}R/\gamma=Ca^{*}$. The inertialess terms, $\sigma_{\alpha\beta,00}$, $\sigma_{\alpha\beta,01}$ and $\sigma_{\alpha\beta,02}^{inertialess}$ (the contribution to $\sigma_{\alpha\beta,02}$ in the absence of inertia) have been previously identified by Mwasame *et al.*[18]. The presence of Z and ζ results in an inertial contribution, $\sigma_{\alpha\beta,02}^{inertial}$, that needs to be added to the inertialess contribution to $\sigma_{\alpha\beta,02}$ such that

$$\sigma_{\alpha\beta,02}=\frac{1}{2}\frac{d^{2}\sigma_{\alpha\beta}}{d\tau_{c}^{2}}\bigg|_{\substack{\tau_{C}=0\\ \hat{Z}=0}}=\sigma_{\alpha\beta,02}^{inertialess}+\sigma_{\alpha\beta,02}^{inertial}\,. \tag{39}$$

These additional contributions to the stress in the asymptotic limit can be readily computed from Eqs. (35) -(37) by using an expansions for $\overline{w}_{\alpha\beta}$ and $C_{\alpha\beta}$, similar to Eq. (38), leading to

$$\sigma_{\alpha\beta,02}^{inertial}=\frac{8\phi\Gamma\zeta\left(1-\xi\right)^{2}}{\left(a_{1}+a_{2}+a_{3}\right)^{2}\left(A_{1}+A_{2}\right)}\left(\Omega_{\alpha\gamma}\cdot D_{\gamma\beta}-D_{\alpha\gamma}\cdot\Omega_{\gamma\beta}\right)+\phi\Gamma\left(\frac{\left(1-\xi\right)}{2\left(a_{1}+a_{2}+a_{3}\right)}+2\xi\right)\hat{Z}\frac{DD_{\alpha\beta}}{Dt}\,. \tag{40}$$

Additional details on how to carry out the asymptotic analysis can be found in Mwasame *et al.*[18] Subsequently, the full asymptotic expansion of Eq. (37), patterned on the form of Eq. (1), is given explicitly in vector-tensor form as

$$\underline{\underline{\sigma}} = 2\mu\underline{\underline{\mathrm{D}}} + \phi\mu P(\lambda)2\underline{\underline{\mathrm{D}}} + \left(\frac{4\phi\Gamma\tau_C(1-\xi)^2}{(a_1+a_2+a_3)}\right)\underline{\underline{\mathrm{D}}}$$
$$-\left(\frac{2\phi\Gamma(1-\xi)^2}{(a_1+a_2+a_3)^2(A_1+A_2)}\right)\left(\begin{array}{l} 2\left(\frac{D}{Dt}\underline{\underline{\mathrm{D}}} - \left(\underline{\underline{\Omega}}\cdot\underline{\underline{\mathrm{D}}} - \underline{\underline{\mathrm{D}}}\cdot\underline{\underline{\Omega}}\right)\right) \\ -\frac{4(1-\xi)(2a_1+a_2)}{(a_1+a_2+a_3)}\left(\underline{\underline{\mathrm{D}}}\cdot\underline{\underline{\mathrm{D}}} - \frac{\mathrm{tr}\left(\underline{\underline{\mathrm{D}}}\cdot\underline{\underline{\mathrm{D}}}\right)}{3}\underline{\underline{\mathrm{I}}}\right)\end{array}\right)\tau_C^2 \quad ,$$
$$+\left(\frac{4\phi\Gamma\zeta(1-\xi)^2}{(a_1+a_2+a_3)^2(A_1+A_2)}\left(\underline{\underline{\Omega}}\cdot\underline{\underline{\mathrm{D}}} - \underline{\underline{\mathrm{D}}}\cdot\underline{\underline{\Omega}}\right) + \phi\Gamma\left(\frac{(1-\xi)}{2(a_1+a_2+a_3)} + 2\xi\right)\hat{Z}\frac{D\underline{\underline{\mathrm{D}}}}{Dt}\right)\tau_C^2 + O(\tau_C^3)$$

(41)

where $A_1 \equiv \partial h/\partial I_1\big|_{\tau_C=0} = \frac{\omega}{48}(2-\omega)$ and $A_2 \equiv \partial h/\partial I_2\big|_{\tau_C=0} = \frac{\omega}{48}(2+\omega)$ and the recommended value of $\omega = 8/5$ is used[18]. By comparing Eq. (41) to Eq. (1) the following identifications are made:

$$\hat{Z} = \frac{\mathrm{Re}_p^*}{Ca^*}\frac{100\left(27\lambda^2+30\lambda+10\right)(2\lambda+3)}{\left(3000(\lambda+1)+(2\lambda-2)(19\lambda+16)(2\lambda+3)\right)(\lambda+1)} \quad , \tag{42}$$

and

$$\zeta = \frac{\mathrm{Re}_p^*}{\mathrm{Ca}^*}\frac{160\left(3\lambda^2+3\lambda+1\right)}{9(19\lambda+16)^2} \quad . \tag{43}$$

The ratio Re_p^*/Ca^* is the definition of the Laplace number (La) and is related to the Ohnesorge number[42] (Oh) as $Re_p^*/Ca^* \equiv Oh^{-2} = Re_p/Ca$. These two parameter definitions complete the full PITCEE model equations given by Eqs. (24)-(26) together with the relevant auxiliary equations already presented in Section III. F. Following the discussion in Section 2, it is clear that the parameter ζ, as appearing in Eq. (41), is associated with violation of frame invariance. This parameter also plays an important role in determining the sign (and magnitude) of the normal stress in inertial shear flows as it pre-multiplies the term $\left(\underline{\underline{\Omega}}\cdot\underline{\underline{\mathrm{D}}} - \underline{\underline{\mathrm{D}}}\cdot\underline{\underline{\Omega}}\right)$ in Eq. (41).

Even though the use of the inertial variable, $w_{\alpha\beta}$, has a long and venerable history from the study of liquid crystals[35], this work for the first time distinguishes the ways through which micro-inertia can enter a macroscopic model, either directly through the inertial variable $w_{\alpha\beta}$ or indirectly through the parameter ζ. This latter effect is missing even in recent efforts[36] to develop inertial models for dilute viscoelastic polymer blends with volume preserving microstructure based on a direct extension of liquid crystal

theory. Furthermore, the emergence of ζ as a new parameter shows how asymptotic theory can provide guidance and new insights on the appropriate terms that should appear in macroscopic conformation tensor models and provides further confidence in the use of non-equilibrium thermodynamics in developing (inertial) macroscopic models. The focus of the next section is to demonstrate the applicability of the PITCEE model to dilute emulsions where particle inertia effects are important.

V. APPLICATION OF PITCEE MODEL

A. The reduced PITCEE model

The evaluation of the full inertial model equations requires the specification of $R_{\alpha\beta\gamma\varepsilon} \equiv \Lambda^{-1}_{\alpha\beta\gamma\varepsilon}$, with $\Lambda_{\alpha\beta\gamma\varepsilon}$ defined in (29), to complete Eq. (24) (or alternatively Eq. (35)). However, in general, the inversion of a fourth order tensor is a non-trivial task except when performed numerically. Therefore, we seek specialized limits in which the model can be applied without the need for inversion. One such case is the limit of steady or slowly varying flows, i.e. conditions under which the contributions of the inertial variable in Eqs. (35) and (37)through $\hat{Z}Ca^{*2}\, D\overline{w}_{\alpha\beta}/Dt$ are zero or can be neglected. As we shall demonstrate, this steady state approximation allows for a number of important rheological signatures seen in emulsions in the presence of microinertia to be explained. In the limit $\hat{Z}Ca^{*2}\, D\overline{w}_{\alpha\beta}/Dt \to 0$, the model equations (Eqs. (35)-(37)) reduce to an evolution equation for $C_{\alpha\beta}$ provided by

$$\begin{aligned} &\overset{\nabla}{C}_{\alpha\beta} + \xi\left(D_{\alpha\eta}C_{\eta\beta} + C_{\alpha\eta}D_{\eta\beta}\right) + \zeta\left(\Omega_{\alpha\eta}C_{\eta\beta} - C_{\alpha\eta}\Omega_{\eta\beta}\right) = \\ &-\Lambda_{\alpha\beta\gamma\varepsilon}\left(\frac{\delta H}{\delta C_{\gamma\varepsilon}} - \frac{1}{3}C^{-1}_{\gamma\varepsilon}C_{\rho\eta}\frac{\delta H}{\delta C_{\rho\eta}}\right) + \frac{1}{3}C_{\alpha\beta}C^{-1}_{\rho\eta}\Lambda_{\rho\eta\gamma\varepsilon}\left(\frac{\delta H}{\delta C_{\gamma\varepsilon}} - \frac{1}{3}C^{-1}_{\gamma\varepsilon}C_{\nu\mu}\frac{\delta H}{\delta C_{\nu\mu}}\right) \end{aligned} \tag{44}$$

and a stress tensor given

$$\sigma_{\alpha\beta} = Q_{\alpha\beta\gamma\varepsilon}\nabla_{\gamma}v_{\varepsilon} + 2\left(1-\xi\right)\left(C_{\beta\gamma}\frac{\delta H}{\delta C_{\alpha\gamma}} - \frac{1}{3}C_{\rho\eta}\frac{\delta H}{\delta C_{\rho\eta}}\delta_{\alpha\beta}\right), \tag{45}$$

which are written in dimensional form. These limiting equations are important as they allow us to more carefully investigate the role of the inertial parameter ζ. The simplified form of Eq. (44) assumes a homogenous material description as gradients in the conformation tensor are neglected. Note that the

inertial variable $\underline{\underline{\mathrm{W}}}$ no longer enters the governing equations in this limit. The expressions above in Eqs. (44) and (45) can be written more succinctly in tensor notation by using the selections for the phenomenological parameters in Section III F as

$$\frac{D\underline{\underline{\mathrm{C}}}}{Dt}+(\xi-1)\left(\underline{\underline{\mathrm{C}}}\cdot\underline{\underline{\mathrm{D}}}+\underline{\underline{\mathrm{D}}}\cdot\underline{\underline{\mathrm{C}}}\right)+(\zeta-1)\left(\underline{\underline{\Omega}}\cdot\underline{\underline{\mathrm{C}}}-\underline{\underline{\mathrm{C}}}\cdot\underline{\underline{\Omega}}\right)= -\frac{1}{\tau_C}\left\{\begin{array}{l}(\partial h/\partial I_2)\left(a_2\frac{2}{I_2}\left(\left(\frac{I_1}{2}+\frac{I_2^2}{3}\right)\underline{\underline{\mathrm{C}}}-\frac{3}{2}\underline{\underline{\mathrm{C}}}\cdot\underline{\underline{\mathrm{C}}}-I_2\underline{\underline{\mathrm{I}}}\right)+a_3\left(\underline{\underline{\mathrm{C}}}-\frac{3}{I_2}\underline{\underline{\mathrm{I}}}\right)\right)\\+(\partial h/\partial I_1)\left(a_2\left(\frac{I_1}{3}\underline{\underline{\mathrm{C}}}-\frac{I_1}{I_2}\underline{\underline{\mathrm{I}}}\right)+a_3\left(\frac{3}{I_2}\underline{\underline{\mathrm{C}}}\cdot\underline{\underline{\mathrm{C}}}-\frac{I_1}{I_2}\underline{\underline{\mathrm{C}}}\right)\right)\end{array}\right\}, \quad (46)$$

and

$$\underline{\underline{\sigma}}=2\mu\underline{\underline{\mathrm{D}}}+\phi P(\lambda)\underline{\underline{\mathrm{D}}}+2\phi\Gamma(1-\xi)\left\{(\partial h/\partial I_1)\left(\underline{\underline{\mathrm{C}}}-\frac{I_1}{3}\underline{\underline{\mathrm{I}}}\right)+(\partial h/\partial I_2)\left(I_1\underline{\underline{\mathrm{C}}}-\underline{\underline{\mathrm{C}}}\cdot\underline{\underline{\mathrm{C}}}-\frac{2}{3}I_2\underline{\underline{\mathrm{I}}}\right)\right\}, \quad (47)$$

with

$$\underline{\underline{\mathrm{D}}}=\frac{1}{2}\begin{bmatrix}0&\dot\gamma&0\\\dot\gamma&0&0\\0&0&0\end{bmatrix},\ \underline{\underline{\Omega}}=\frac{1}{2}\begin{bmatrix}0&\dot\gamma&0\\-\dot\gamma&0&0\\0&0&0\end{bmatrix}. \quad (48)$$

In these expressions, the related auxiliary expressions are identified as follows (unless otherwise specified): ξ is provided by Eq. (31), a_2 and a_3 by Eq. (32), $P(\lambda)$ by Eq. (33), $(\partial h/\partial I_1)$ by Eq. (20), $(\partial h/\partial I_2)$ by Eq. (21) and ζ is provided by Eq. (43), $\tau_C\equiv Ca^*=\mu R/\gamma$ and $\Gamma=3\gamma/R$. The expressions in Eqs. (46)-(48) (and the corresponding auxiliary expressions) are referred to as the "reduced PITCEE" model and will be the ones used for comparison against experimental data in the following section.

The left hand side of the evolution equation for the conformation tensor in Eq. (46) can be identified as a generalized co-deformational derivative denoted by the short hand $\frac{D^{(\xi,\zeta)}\underline{\underline{\mathrm{C}}}}{Dt}$ as

$$\frac{D^{(\xi,\zeta)}\underline{\underline{\mathrm{C}}}}{Dt}\equiv\frac{D\underline{\underline{\mathrm{C}}}}{Dt}+(\xi-1)\left(\underline{\underline{\mathrm{C}}}\cdot\underline{\underline{\mathrm{D}}}+\underline{\underline{\mathrm{D}}}\cdot\underline{\underline{\mathrm{C}}}\right)+(\zeta-1)\left(\underline{\underline{\Omega}}\cdot\underline{\underline{\mathrm{C}}}-\underline{\underline{\mathrm{C}}}\cdot\underline{\underline{\Omega}}\right). \quad (49)$$

Its introduction goes beyond the traditional non-affine effects modeled through the more standard Gordon-Schowalter derivative[2] which can be recovered from Eq. (49) in the limit $\zeta=0$. The use of Eq.

(44) with $\zeta \neq 0$, as provided, for example, by Eq. (43), allows for the introduction of micro-inertia effects into the model equations without the need of additional variables and therefore of a substantial more complexity into the model equations. The presence of a non-zero ξ parameter also makes $D^{(\xi,\zeta)}\underline{\underline{C}}/Dt$ and therefore the whole model to be non-objective.

B. Comparison of the reduced PITCEE model predictions against numerical simulation data

The predictions of the reduced PITCEE model equations are compared against steady shear simulation data by Li and Sarkar[22] for $\lambda = 1$ in Fig. 2. Also shown in the same figure are the predictions of the asymptotic theory of Eq. (1) for the scaled second normal stress difference: note that the first normal stress difference predicted by Eq. (1) is in full agreement with that predicted by the reduced PITCEE model and therefore is not explicitly shown in the same figure. The discrepancy between the predictions of asymptotic theory and the reduced PITCEE model for N_1/σ_{12} is as a consequence of the fact that the former are strictly speaking limited to the infinitesimal capillary limit. The key result seen in Fig. 2 is that the reduced PITCEE model equations can produce a change in sign of the normal stress differences as the Reynolds number increases, similar to what is seen in the independent simulation data, because ζ depends on the Oh number. Furthermore, the model predictions are in semi-quantitative agreement with those microscopic simulation data, exhibiting all the key features of the rheology data, and most importantly a change in the sign of normal stress differences following a change in the orientation of the drop from $\theta < 45^0$ to $\theta > 45^0$. Remarkably, all these predictions are made possible through the use of the generalized Gordon-Schowalter time derivative in Eq. (49), without the use of any additional inertial variable $\underline{\underline{W}}$. Note that the disagreement between the model predictions and experimental data can be attributed to the fact that the parameter ζ in Eq. (43) is developed based on asymptotic theory that is strictly valid only for small Re_p. On the other hand, note under the constraint $\zeta = 0$, the PITCEE Eq. (49) reduces to the inertialess TCEE model and is unable to capture the effects of microinertia as the capillary number is the only relevant dimensionless group in that limit. Similar limitations are also seen if the model of Maffetone and Minale[7] is used to describe data in the presence of microinertia. This result is not surprising as in the absence of the parameter ζ the only dimensionless number in the model is the capillary number, which is a constant for the prescribed experiments. As a consequence, the model predictions are insensitive to the prevailing value of the particle Reynolds number. This insensitivity

highlights a clear limitation of current emulsion flow models that are also developed in the limit of zero particle inertia. Accounting for the effects of particle scale inertia clearly requires the use of the full extended time derivative in Eq. (49). Moreover, the present analysis also highlights that at steady-state particle inertia effects can be introduced effectively into the flow model through the parameter ζ alone.

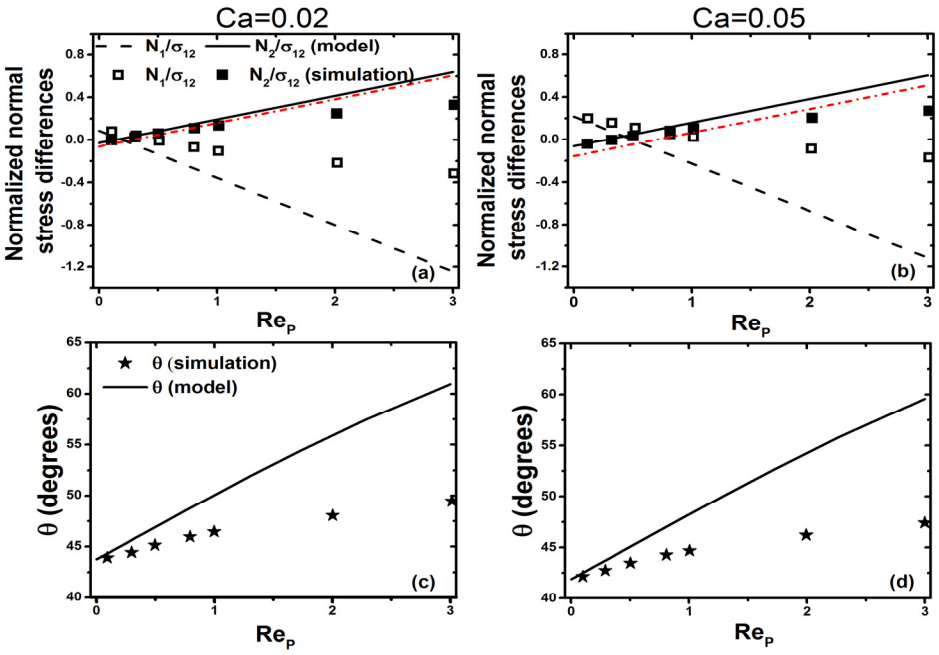

FIGURE 2. The relationship between (a, b) the normalized normal stress differences and (c, d) the orientation of an emulsion droplet relative to the flow direction as a function of particle Reynolds number in steady simple shear flow at two different capillary numbers (a, c) 0.02 and (b, d) 0.05 and for $\lambda = 1$ from both simulation (symbols) from Li and Sarkar[22] and the reduced PITCEE model predictions (lines). The dash-dotted lines in (a) and (b) correspond to the predictions of the asymptotic theory of Raja *et al*.[23] shown in Eq. (1) for N_1/σ_{12} (note that the corresponding predictions for N_2/σ_{12} overlay with those of the reduced PITCEE model and are therefore not shown). In the PITCEE model predictions shown, the value of ζ is selected based on Eq. (43). Note that the interfacial stress predictions from the PITCEE model shown are computed from Eq. (28) but by neglecting any viscous contribution (i.e. ignoring the first term in Eq. (47)).

An even better quantitative agreement with the simulation data can be achieved through the reduced PITCEE model by non-linearly extending Eq. (43) in the Oh number, for example, as shown in the following ansatz:

$$\zeta = \frac{1}{Oh^2}\frac{160\left(3\lambda^2+3\lambda+1\right)}{9\left(19\lambda+16\right)^2}\left(\frac{1}{1+1/Oh^2}\right)^p \quad . \tag{50}$$

It is possible to use this expression for ζ that contains just one adjustable parameter p to fit the data shown in Fig. 2. Crucially, this expression reduces to Eq. (43) in the limit of small Oh. The model predictions using this extended form of ζ for $p = 0.23$ are presented in Fig. 4 showing good agreement with simulation data of Li and Sarkar[22]. The possibility of obtaining better quantitative agreement using the full PITCEE model equations by including the inertial variable $\underline{\underline{w}}$ and $R_{\alpha\beta\gamma\varepsilon} \equiv \Lambda^{-1}_{\alpha\beta\gamma\varepsilon}$ will be explored in a future publication. Finally, it is worth noting that both the simulation data of Li and Sarkar[22] as well as the model Eqs. (46) and (47) (but ignoring the first term in Eq. (47)) follow the correlation of Jansseune *et al.*[43] for the interfacial stresses for $\lambda = 1$ given by

$$\frac{N_1}{\sigma_{12}} \equiv \frac{(\sigma_{11} - \sigma_{22})}{\sigma_{12}} = 2cot(2\theta) \ . \tag{51}$$

This expression is independent of any underlying model assumption and is directly obtained from the stress expression of Batchelor[44] by considering only the structural contribution from the elastic interface of the emulsion droplet[43].

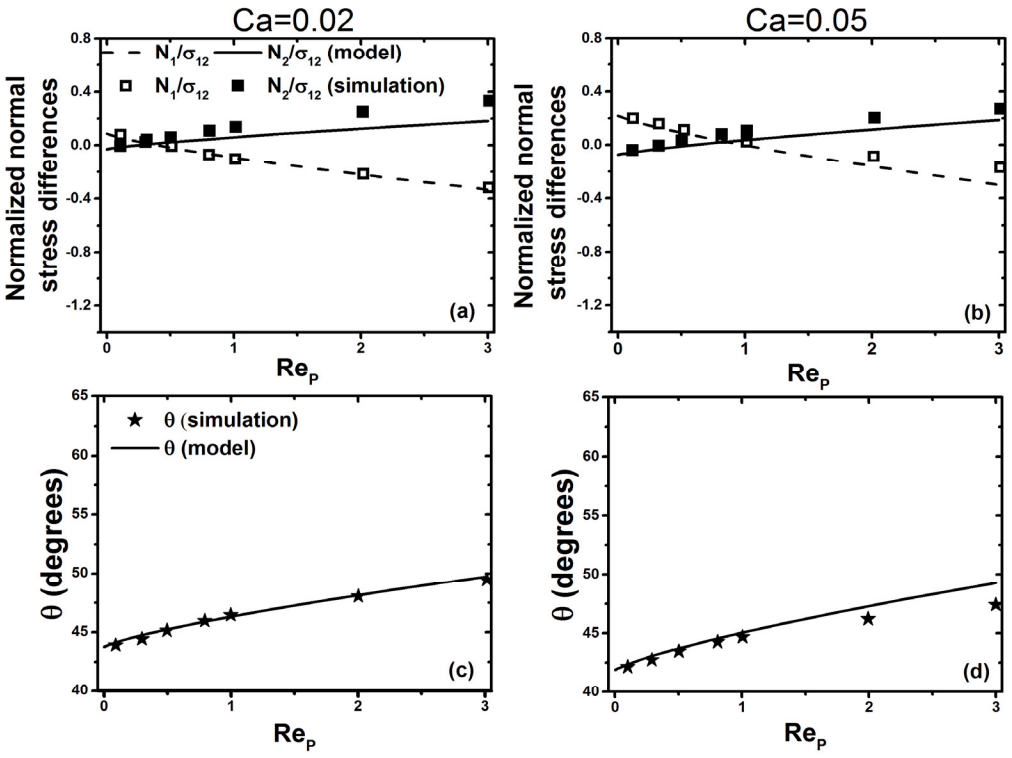

FIGURE 3. The relationship between (a, b) the normalized normal stress differences and (c, d) the orientation of an emulsion droplet relative to the flow direction as a function of particle Reynolds number in steady simple shear flow at two different capillary numbers (a, c) 0.02 and (b, d) 0.05 and for $\lambda = 1$ from

both simulation (symbols) from Li and Sarkar[22] and the reduced PITCEE model predictions (lines) considering ζ is provided by Eq. (50) for $p = 0.23$. Note that the interfacial stress predictions from the PITCEE model shown are computed from Eq. (28) but by neglecting any viscous contribution (i.e. ignoring the first term in Eq. (47)).

A word of caution is warranted here. Although the model can be non-linearly extended to describe the rheology at larger Re_p (for example, as shown through Eq. (50)) the physical interpretation of the conformation tensor at higher particle Reynolds numbers may be different. Unlike the limit of zero particle inertia where the conformation tensor unambiguously represents the emulsion droplet microstructure, at larger Re_p the conformation tensor should be considered as an effective descriptor of anisotropy in the fluid arising from both the deformed emulsion droplet and micro-inertia effects arising from the matrix fluid surrounding the droplet. Furthermore, even when $\mathrm{Re}_p < 1$, the Laplace number can be large and consequently the asymptotic results on which the PITCEE model depends upon may be inadequate. This may be critical in explaining the inability of the PITCEE model to correctly capture the inertial-induced changes to the shear stress as observed by Li and Sarkar[22] (not shown here), despite the successes of the model in capturing the inertial-induced changes to the ratios of the normal stress to the shear stress and the droplet orientation, as shown in Figs. 2 and 3. It is anticipated that to achieve this higher level of quantitative predictive capability of the model at the large Laplace values corresponding to the Li and Sarkar's experimental conditions, it requires further fine-tuning of the non-linear dependence of model parameters other than the ζ to the Laplace (or, equivalently, Ohnesorge) number. However, as this requires further simulation data results (especially on transients) that are not available currently, it is relegated for a future study. Nevertheless, the power of the conformation tensor-based PITCEE model is that it provides a framework through which the results from asymptotic theory can be smoothly extended to much larger particle Reynolds numbers with only assumption that a general tensor inner variable can describe the structural anisotropy induced by the flow. Most importantly, the key result of this section is that the most important qualitative effects of particle inertia at steady state flows, those observed on the sign changes of the normal stresses and in the droplet orientation, can be accommodated without the need of the inertial variable $\underline{\underline{w}}$ by simply extending the corresponding inertialess model equations through the use of a second non-affine parameter that affects the rotation of the droplets. Those effects can be independently measured subjecting the sample to additional solid body rotation.

VI. CONCLUSIONS

This work has outlined the systematic, thermodynamically consistent, development of a general macroscopic, conformation tensor-based model for emulsion rheology, the PITCEE model, that also incorporates particle inertia effects. When those inertia effects are absent, the equations are reduced consistently to the previously developed inertialess TCEE model[18], which is also used to here to recover most of the new model parameters. The remaining two PITCEE model parameters are evaluated using existing asymptotic theories that capture the lowest order inertial effects[23]. This approach towards the development of macroscopic models by utilizing results from microscopic analysis is a powerful one and sets a new paradigm in multiscale analysis and modeling. Asymptotic results enable the development of macroscopic material flow models without the need of any adjustable parameters. Simultaneously, macroscopic models, constructed systematically within a rigorous thermodynamic framework, may significantly extend the range of validity of asymptotic relations and/or provide the means for a much more effective extension with significantly reduced number of additional adjustable parameters.

The resultant inertial macroscopic model developed in this work, the PITCEE model, is capable of capturing all known limiting behaviors at small Reynolds and Capillary numbers, and the resultant model predictions are validated by comparison against recent simulation results[22]. In addition, the capability to develop the inertial PITCEE model based on non-equilibrium thermodynamics provides further validation of the bracket approach and underlines the importance of developing self-consistent models. Away from the asymptotic limits that the theory has been rigorously developed from, the PITCEE model predictions only show qualitative agreement with experiments. However, in this case, the introduction of correction terms with minimal adjustable parameters (just one in our case) can significantly improve the accuracy of the model predictions. Further improvements to the quantitative predictions of the model can be achieved by fine-tuning of the model parameters but this requires additional simulation data and is relegated to future work.

A critical outcome of this work is the introduction of a new co-deformational time derivative that incorporates two non-affine parameter ξ and ζ. ξ is traditionally associated with non-affine motion[2, 3] and from matching the macroscopic model to asymptotic solutions, ζ is clearly related to the Ohnesorge number in the case of emulsion droplets. As a result, it may be an important additional parameter in modeling suspensions that are in the small Reynolds number regime and at small Capillary numbers. As demonstrated in this work, instances of such particulate suspensions exist and provide further justification for the efforts in developing inertial macroscopic models. Interestingly, from a thermodynamics

perspective, ζ can take on any value, and therefore, provides a new modeling paradigm to describing complex fluids and structured soft matter under flows for which microinertia is important. More generally, the co-deformational derivative developed in this work may be applicable to other systems.

ACKNOWLEDGMENTS

This material is based upon work supported by the National Science Foundation under Grant No. CBET 312146. Any opinions, findings, and conclusions or recommendations expressed in this material are those of the author(s) and do not necessarily reflect the views of the National Science Foundation.

References

1. J. Oldroyd, *On the formulation of rheological equations of state* (The Royal Society, 1950).
2. R. Gordon, and W. Schowalter, "Anisotropic fluid theory: a different approach to the dumbbell theory of dilute polymer solutions," Transactions of the Society of Rheology **16**, 79 (1972).
3. M. Johnson, and D. Segalman, "A model for viscoelastic fluid behavior which allows non-affine deformation," Journal of Non-Newtonian Fluid Mechanics **2**, 255 (1977).
4. C.-J. Lin, J. H. Peery, and W. Schowalter, "Simple shear flow round a rigid sphere: inertial effects and suspension rheology," Journal of Fluid Mechanics **44**, 1 (1970).
5. H. Haddadi, and J. F. Morris, "Microstructure and rheology of finite inertia neutrally buoyant suspensions," Journal of Fluid Mechanics **749**, 431 (2014).
6. H. Haddadi, and J. F. Morris, "Topology of pair-sphere trajectories in finite inertia suspension shear flow and its effects on microstructure and rheology," Physics of Fluids **27**, 043302 (2015).
7. P. Maffettone, and M. Minale, "Equation of change for ellipsoidal drops in viscous flow," Journal of Non-Newtonian Fluid Mechanics **78**, 227 (1998).
8. E. D. Wetzel, and C. L. Tucker, "Area tensors for modeling microstructure during laminar liquid-liquid mixing," International journal of multiphase flow **25**, 35 (1999).
9. E. D. Wetzel, and C. L. Tucker, "Droplet deformation in dispersions with unequal viscosities and zero interfacial tension," Journal of Fluid Mechanics **426**, 199 (2001).
10. M. Doi, and T. Ohta, "Dynamics and rheology of complex interfaces. I," The Journal of chemical physics **95**, 1242 (1991).
11. B. J. Edwards, and M. Dressler, "A rheological model with constant approximate volume for immiscible blends of ellipsoidal droplets," Rheologica Acta **42**, 326 (2003).
12. M. Dressler, and B. J. Edwards, "The influence of matrix viscoelasticity on the rheology of polymer blends," Rheologica Acta **43**, 257 (2004).
13. M. Grmela, M. Bousmina, and J.-F. Palierne, "On the rheology of immiscible blends," Rheologica Acta **40**, 560 (2001).
14. W. Yu, M. Bousmina, M. Grmela, J.-F. Palierne, and C. Zhou, "Quantitative relationship between rheology and morphology in emulsions," Journal of Rheology **46**, 1381 (2002).
15. A. Ait-Kadi, A. Ramazani, M. Grmela, and C. Zhou, ""“Volume preserving” rheological models for polymer melts and solutions using the GENERIC formalism," Journal of Rheology **43**, 51 (1999).
16. M. Grmela, A. Ammar, F. Chinesta, and G. Maîtrejean, "A mesoscopic rheological model of moderately concentrated colloids," Journal of Non-Newtonian Fluid Mechanics **212**, 1 (2014).
17. M. Minale, "Models for the deformation of a single ellipsoidal drop: a review," Rheologica Acta **49**, 789 (2010).

18. P. M. Mwasame, N. J. Wagner, and A. N. Beris, "On the macroscopic modeling of dilute emulsions under flow," Journal of Fluid Mechanics **831**, 433 (2017).
19. P. M. Kulkarni, and J. F. Morris, "Suspension properties at finite Reynolds number from simulated shear flow," Physics of Fluids **20**, 040602 (2008).
20. A. Nicolas, J.-L. Barrat, and J. Rottler, "Effects of inertia on the steady-shear rheology of disordered solids," Physical review letters **116**, 058303 (2016).
21. E. Linares-Guerrero, M. L. Hunt, and R. Zenit, "Effects of inertia and turbulence on rheological measurements of neutrally buoyant suspensions," Journal of Fluid Mechanics **811**, 525 (2017).
22. X. Li, and K. Sarkar, "Effects of inertia on the rheology of a dilute emulsion of drops in shear," Journal of Rheology **49**, 1377 (2005).
23. R. V. Raja, G. Subramanian, and D. L. Koch, "Inertial effects on the rheology of a dilute emulsion," Journal of Fluid Mechanics **646**, 255 (2010).
24. S. Farokhirad, T. Lee, and J. F. Morris, "Effects of inertia and viscosity on single droplet deformation in confined shear flow," Communications in Computational Physics **13**, 706 (2013).
25. P. Srivastava, A. R. Malipeddi, and K. Sarkar, "Steady shear rheology of a viscous emulsion in the presence of finite inertia at moderate volume fractions: sign reversal of normal stress differences," Journal of Fluid Mechanics **805**, 494 (2016).
26. W. Schowalter, C. Chaffey, and H. Brenner, "Rheological behavior of a dilute emulsion," Journal of Colloid and Interface Science **26**, 152 (1968).
27. C. E. Chaffey, and H. Brenner, "A second-order theory for shear deformation of drops," Journal of Colloid and Interface Science **24**, 258 (1967).
28. S. Torza, R. Cox, and S. Mason, "Particle motions in sheared suspensions XXVII. Transient and steady deformation and burst of liquid drops," Journal of Colloid and Interface Science **38**, 395 (1972).
29. T. G. Mezger, *The rheology handbook: for users of rotational and oscillatory rheometers* (Vincentz Network GmbH & Co KG, 2006).
30. N. Frankel, and A. Acrivos, "The constitutive equation for a dilute emulsion," Journal of Fluid Mechanics **44**, 65 (1970).
31. D. Barthes-Biesel, and A. Acrivos, "Deformation and burst of a liquid droplet freely suspended in a linear shear field," Journal of Fluid Mechanics **61**, 1 (1973).
32. J. Rallison, "Note on the time-dependent deformation of a viscous drop which is almost spherical," Journal of Fluid Mechanics **98**, 625 (1980).
33. F. M. Leslie, "Some constitutive equations for anisotropic fluids," The Quarterly Journal of Mechanics and Applied Mathematics **19**, 357 (1966).
34. J. Ericksen, "Anisotropic fluids," Archive for Rational Mechanics and Analysis **4**, 231 (1959).
35. A. N. Beris, and B. J. Edwards, *Thermodynamics of flowing systems: with internal microstructure* (Oxford University Press on Demand, 1994).
36. M. Dressler, "Inertial theories for dilute viscoelastic polymer blends with a volume preserving microstructure," Journal of Non-Newtonian Fluid Mechanics **173**, 40 (2012).
37. G. Ryskin, and J. Rallison, "The extensional viscosity of a dilute suspension of spherical particles at intermediate microscale Reynolds numbers," Journal of Fluid Mechanics **99**, 513 (1980).
38. R. B. Bird, R. C. Armstrong, and O. Hassager, "Dynamics of polymeric liquids. Vol. 1: Fluid mechanics," (1987).
39. R. G. Larson, *Constitutive Equations for Polymer Melts and Solutions: Butterworths Series in Chemical Engineering* (Butterworth-Heinemann, 1988).
40. D. Xu, J. Cui, R. Bansal, X. Hao, J. Liu, W. Chen, and B. S. Peterson, "The ellipsoidal area ratio: an alternative anisotropy index for diffusion tensor imaging," Magnetic resonance imaging **27**, 311 (2009).
41. B. Edwards, M. Dressler, M. Grmela, and A. Ait-Kadi, "Rheological models with microstructural constraints," Rheologica acta **42**, 64 (2003).

42. G. H. McKinley, and M. Renardy, "Wolfgang von ohnesorge," Physics of Fluids **23**, 127101 (2011).
43. T. Jansseune, J. Mewis, P. Moldenaers, M. Minale, and P. Maffettone, "Rheology and rheological morphology determination in immiscible two-phase polymer model blends," Journal of Non-Newtonian Fluid Mechanics **93**, 153 (2000).
44. G. Batchelor, "The stress system in a suspension of force-free particles," Journal of Fluid Mechanics **41**, 545 (1970).

APPENDIX A

This appendix presents the general PITCEE model equations in properly non-dimensional and tensorial form. For that note that the 'hat' symbol is used to denote dimensionless quantities (note however that $C_{\alpha\beta}$ is already defined to be dimensionless) and that we use the following scales:

1. For the time we use everywhere the capillary relaxation time, $\tau_C = Ca^* = \mu R / \gamma$. Correspondingly, the dimensionless time τ is defined from t as

$$\tau = t / Ca^* . \tag{52}$$

This also means that any time derivatives (like the rate of strain and vorticity tensors, $D_{\alpha\beta}$ and $\Omega_{\alpha\beta}$, respectively, the upper convected time derivative for the conformation tensor, $\overset{\nabla}{C}_{\alpha\beta}$ and the scaled structural momentum tensor $\overline{w}_{\alpha\beta}$, scale like the inverse capillary relaxation time, $1/\tau_C = 1/Ca^* = \gamma/\mu R$ whereas any second derivatives, like the upper convected time derivative of the scaled structural momentum tensor, $\overset{\nabla}{\overline{w}}_{\alpha\beta}$ scale like the inverse capillary relaxation time square, $1/\tau_C^2 = 1/(Ca^*)^2 = \gamma^2/\mu^2 R^2$. A consequence of this scaling is that the dimensionless shear rate becomes simply the capillary number $Ca = Ca^* \dot{\gamma}$.

2. For the Volterra derivative of the Hamiltonian with respect to the conformation tensor, $\delta H / \delta \underline{\underline{C}}$ we use $\phi\Gamma = \phi\gamma / R$ such that the dimensionless Volterra derivative becomes

$$\frac{\delta \hat{H}}{\delta \underline{\underline{C}}} = \frac{\delta H}{\delta \underline{\underline{C}}} \Big/ (\phi\Gamma) . \tag{53}$$

3. For the inertial parameter, Z we use $Ca^* \mu\phi$. In this way the dimensionless inertial parameter becomes

$$\hat{Z} = Z / (\phi\Gamma Ca^{*2}) . \tag{54}$$

4. For the fourth order relaxation tensor, $\underline{\underline{\underline{\underline{\Lambda}}}}$ we use $1/(\tau_C \phi \dot{\Gamma})$. In this way, for its inverse, the fourth order relaxation tensor $R_{\alpha\beta\gamma\varepsilon}$ we use the inverse scaling $\tau_C \phi \dot{\Gamma}$. The dimensionless fourth order relaxation tensor becomes

$$\hat{\underline{\underline{\underline{\underline{\mathrm{R}}}}}}^{-1} = \hat{\underline{\underline{\underline{\underline{\Lambda}}}}} = \underline{\underline{\underline{\underline{\Lambda}}}} \phi \dot{\Gamma} Ca^* \,. \tag{55}$$

where the dimensionless parameters α_1, α_2 are still provided by Eqs. (32). Also, the remaining dimensionless parameters, ξ, ζ are still provided by the same equations, Eqs. (31) and (43).

6. Finally for the inertial variable, we use Ca^*. In this way the dimensionless inertial parameter becomes

$$\hat{\underline{\underline{\mathrm{w}}}} = Ca^* \underline{\underline{\mathrm{w}}} \,. \tag{56}$$

Based on this non-dimensionalization, the final equation for the time evolution of the dimensionless structural momentum tensor, Eq. (35), now becomes:

$$\hat{\underline{\underline{\underline{\underline{\Lambda}}}}} : \left(\hat{Z} \frac{D\hat{\underline{\underline{\mathrm{w}}}}}{D\tau} + \frac{\delta \hat{H}}{\delta \underline{\underline{\mathrm{C}}}} - \frac{1}{3} \left(\underline{\underline{\mathrm{C}}} : \frac{\delta \hat{H}}{\delta \underline{\underline{\mathrm{C}}}} \right) \underline{\underline{\mathrm{C}}}^{-1} \right) = -\left(\hat{\underline{\underline{\mathrm{w}}}} + \xi \left(\underline{\underline{\mathrm{C}}} \cdot \hat{\underline{\underline{\mathrm{D}}}} + \hat{\underline{\underline{\mathrm{D}}}} \cdot \underline{\underline{\mathrm{C}}} \right) + \zeta \left(\hat{\underline{\underline{\Omega}}} \cdot \underline{\underline{\mathrm{C}}} - \underline{\underline{\mathrm{C}}} \cdot \hat{\underline{\underline{\Omega}}} \right) \right) \,, \tag{57}$$

while Eq. (36) which describes the evolution of the conformation tensor simplifies to

$$\frac{D\underline{\underline{C}}}{D\tau} - \left(\underline{\underline{C}} \cdot \hat{\underline{\underline{D}}} + \hat{\underline{\underline{D}}} \underline{\underline{C}} \right) - \left(\hat{\underline{\underline{\Omega}}} \underline{\underline{C}} - \underline{\underline{C}} \hat{\underline{\underline{\Omega}}} \right) + \frac{\left(\underline{\underline{C}}^{-1} : \left(\hat{\underline{\mathrm{v}}} \cdot \underline{\nabla} \right) \underline{\underline{C}} \right)}{3} \underline{\underline{C}} = \hat{\underline{\underline{w}}} - \frac{\left(\underline{\underline{C}}^{-1} : \hat{\underline{\underline{w}}} \right)}{3} \underline{\underline{C}} \,. \tag{58}$$

In these expressions, all parameters and all variables are now dimensionless. Most notably, Eqs. (54), (55) , in combination with Eqs. (42) and (29), (32) can be used to define parametrically as a function of the viscosity ratio λ the dimensionless parameters $\hat{Z}, \hat{\underline{\underline{\underline{\underline{\Lambda}}}}}$, respectively, while Eqs. (31) and (43) for the dimensionless parameters ξ, ζ. Moreover, the dimensionless Volterra derivative of the Hamiltonian with respect to the conformation tensor is now equal to

$$\frac{\delta \hat{H}}{\delta \underline{\underline{\mathrm{C}}}} = \left(\left(\partial h / \partial I_1 \right) \left(\underline{\mathrm{I}} - \left(\frac{I_2}{I_2^2 - 2I_1} \right) \underline{\underline{\mathrm{C}}}^{-1} \right) + \left(\partial h / \partial I_2 \right) \left(I_1 \underline{\mathrm{I}} - \underline{\underline{\mathrm{C}}} - \left(\frac{I_1 I_2 - 3}{I_2^2 - 2I_1} \right) \underline{\underline{\mathrm{C}}}^{-1} \right) \right) \,. \tag{59}$$

Finally, note that for a simple shear flow we now have the following expressions for the dimensionless rate of strain and vorticity tensors

$$\hat{\underline{\underline{\mathrm{D}}}} = \frac{1}{2}\begin{bmatrix} 0 & Ca & 0 \\ Ca & 0 & 0 \\ 0 & 0 & 0 \end{bmatrix}$$
$$\hat{\underline{\underline{\Omega}}} = \frac{1}{2}\begin{bmatrix} 0 & Ca & 0 \\ -Ca & 0 & 0 \\ 0 & 0 & 0 \end{bmatrix} \quad (60)$$

If we look carefully between the set of Eqs. (57),(58) and (24),(25) they are identical; only the interpretation of the parameters is different, all of them being replaced in the first set, as indicated above, by their dimensionless equivalents. It is really therefore the new dimensionless parameter $\hat{Z}$ that one can compare against the ζ parameter; and from what we see from that comparison both have the same order of magnitude with actually the first one being typically larger than the second. Both Eqs. (57) and (58) need to therefore to be integrated in time subject to appropriate initial conditions in order to provide us with the system's time evolution subject to a given velocity field history. However, for steady sate or slowly varying flows for which the material time derivative $\frac{D\hat{\underline{\underline{\mathrm{w}}}}}{D\tau}$ is zero or small enough to be neglected the terms weighted by *Z* are zero or can be neglected, respectively, thus giving rise to the reduced PITCEE model equations as indicated in Section V.A above.

Low Re_p

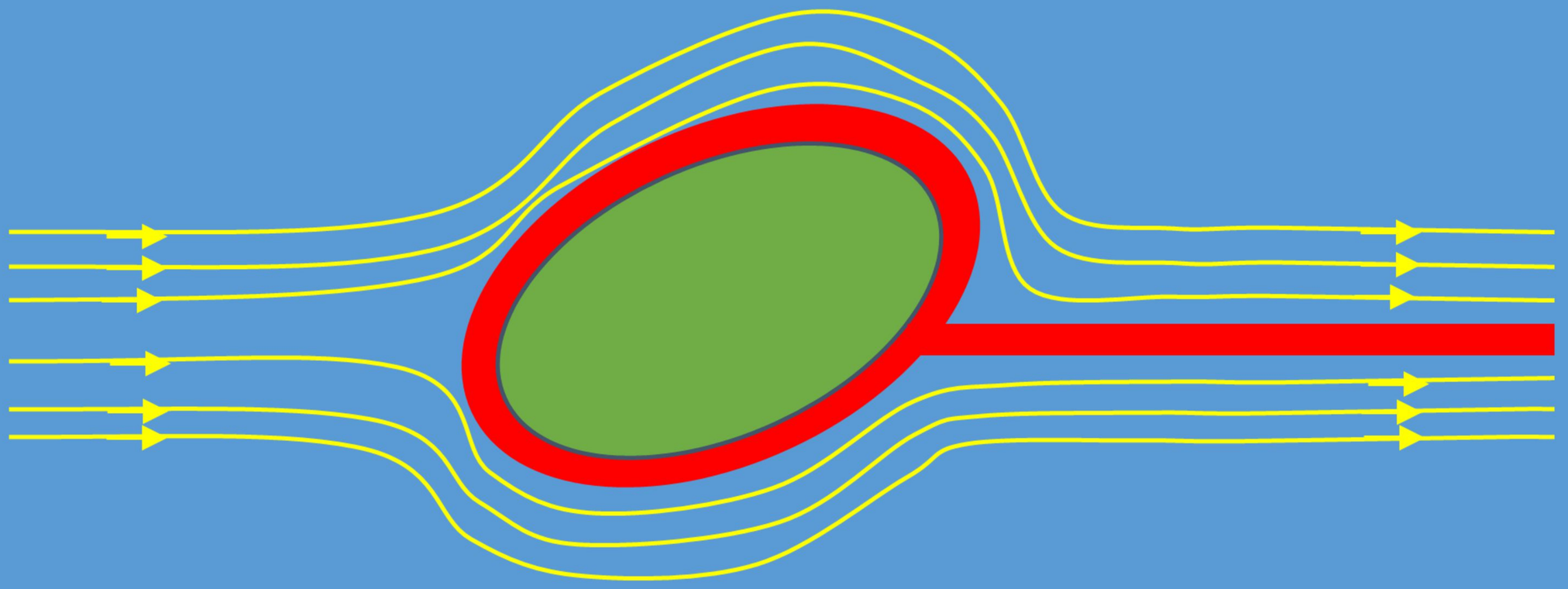

Finite Re_p

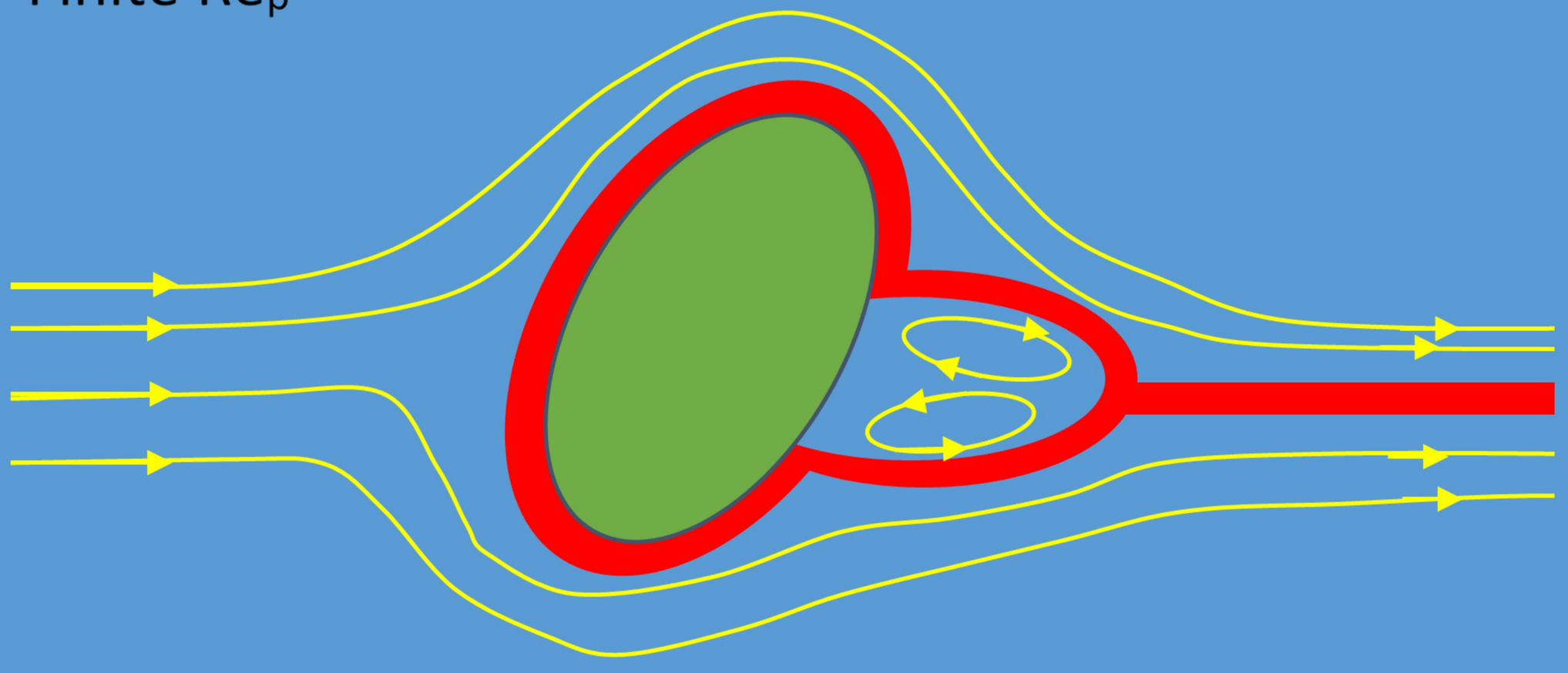

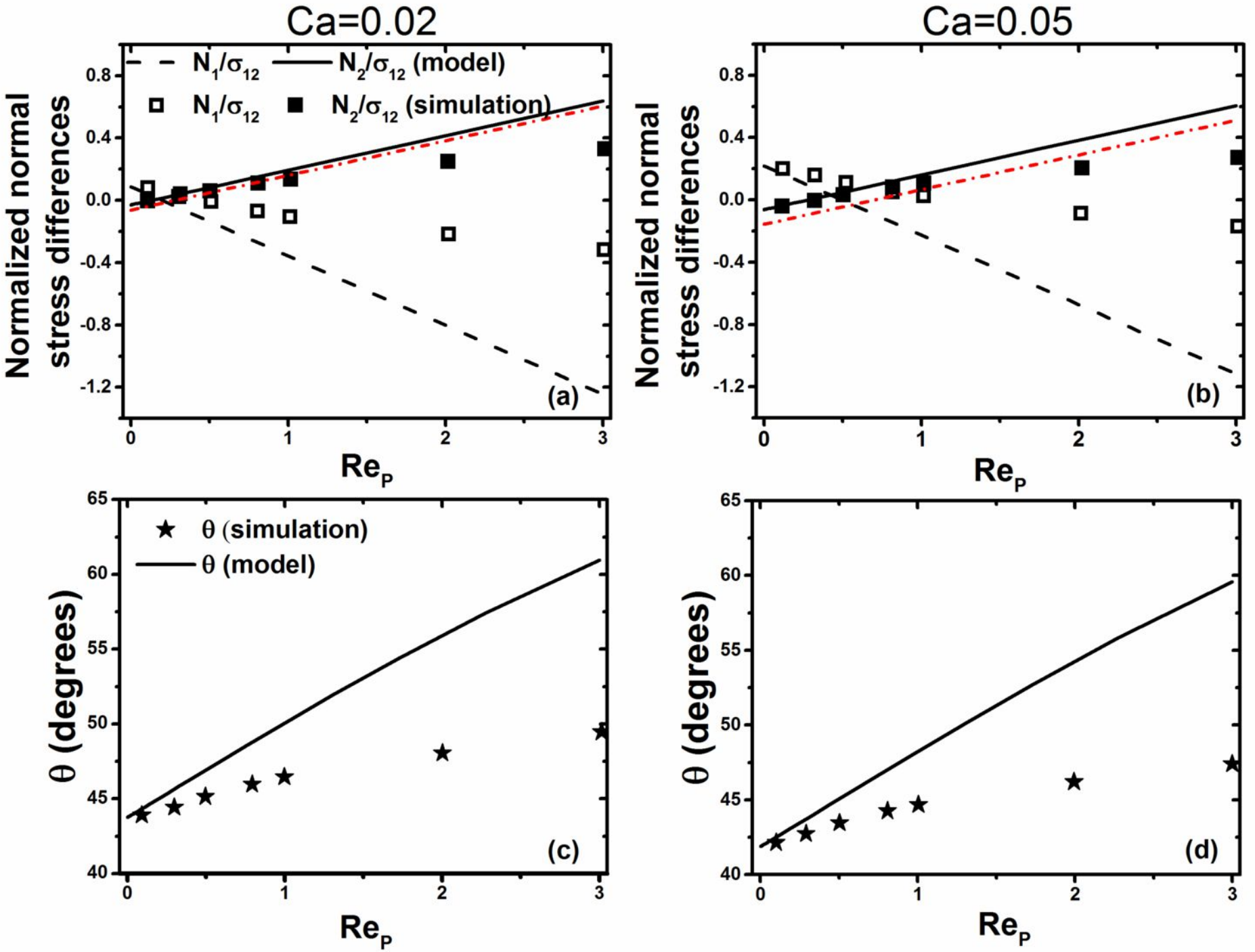
Ca=0.02
Ca=0.05
N1/σ12
N2/σ12 (model)
N1/σ12
N2/σ12 (simulation)
Normalized normal stress differences
ReP
(a)
(b)
θ (simulation)
θ (model)
θ (degrees)
(c)
(d)

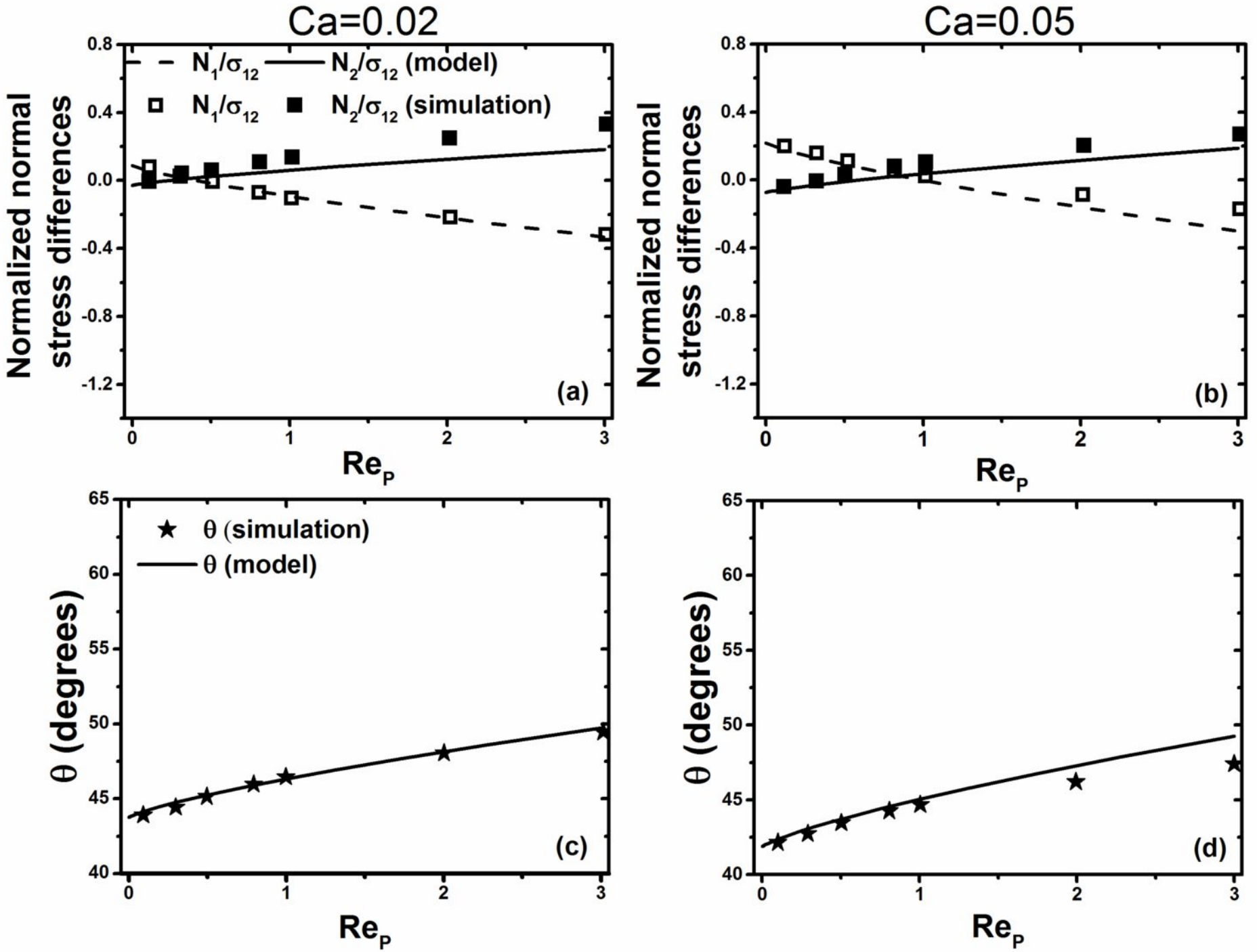
Ca=0.02
Ca=0.05
Normalized normal stress differences
N_1/σ_{12}
N_2/σ_{12} (model)
N_1/σ_{12}
N_2/σ_{12} (simulation)
(a)
(b)
Re_P
θ (degrees)
θ (simulation)
θ (model)
(c)
(d)